282, 30022–30028
22. Kitamoto, T., Ohta, M., Doh-ura, K., Hitoshi, S., Terao, Y., and Tateishi, J. (1993) *Biochem. Biophys. Res. Commun.* **191,** 709–714
23. Taguchi, Y., Mohri, S., Ironside, J. W., Muramoto, T., and Kitamoto, T. (2003) *Am. J. Pathol.* **163,** 2585–2593
24. Kitamoto, T., Muramoto, T., Mohri, S., Doh-ura, K., and Tateishi, J. (1991) *J. Virol.* **65,** 6292–6295
25. Kitamoto, T., Muramoto, T., Hilbich, C., Beyreuther, K., and Tateishi, J. (1991) *Brain Res.* **545,** 319–321
26. Grathwohl, K. U., Horiuchi, M., Ishiguro, N., and Shinagawa, M. (1996) *Arch. Virol.* **141,** 1863–1874
27. Bishop, M. T., Hart, P., Aitchison, L., Baybutt, H. N., Plinston, C., Thomson, V., Tuzi, N. L., Head, M. W., Ironside, J. W., Will, R. G., and Manson, J. C. (2006) *Lancet Neurol.* **5,** 393–398
28. Asante, E. A., Linehan, J. M., Gowland, I., Joiner, S., Fox, K., Cooper, S., Osiguwa, O., Gorry, M., Welch, J., Houghton, R., Desbruslais, M., Brandner, S., Wadsworth, J. D., and Collinge, J. (2006) *Proc. Natl. Acad. Sci. U. S. A.* **103,** 10759–10764
29. Yamada, M., and the Variant CJD Working Group Creutzfeldt-Jakob Disease Surveillance Committee, Japan (2006) *Lancet* **367,** 874
30. Saborio, G. P., Permanne, B., and Soto, C. (2001) *Nature* **411,** 810–813
31. Jones, M., Peden, A. H., Prowse, C. V., Groner, A., Manson, J. C., Turner, M. L., Ironside, J. W., MacGregor, I. R., and Head, M. W. (2007) *J. Pathol.* **213,** 21–26
32. Korth, C., Kaneko, K., Groth, D., Heye, N., Telling, G., Mastrianni, J., Parchi, P., Gambetti, P., Will, R., Ironside, J. W., Heinrich, C., Tremblay, P., DeArmond, S. J., and Prusiner, S. B. (2003) *Proc. Natl. Acad. Sci. U. S. A.* **100,** 4784–4789
33. Tahiri-Alaoui, A., Sim, V. L., Caughey, B., and James, W. (2006) *J. Biol. Chem.* **281,** 34171–34178
34. Baskakov, I. V., Legname, G., Baldwin, M. A., Prusiner, S. B., and Cohen, F. E. (2002) *J. Biol. Chem.* **277,** 21140–21148
35. Meier, P., Genoud, N., Prinz, M., Maissen, M., Rulicke, T., Zurbriggen, A., Raeber, A. J., and Aguzzi, A. (2003) *Cell* **113,** 49–60
36. Bellinger-Kawahara, C. G., Kempner, E., Groth, D., Gabizon, R., and Prusiner, S. B. (1988) *Virology* **164,** 537–541
37. Kocisko, D. A., Come, J. H., Priola, S. A., Chesebro, B., Raymond, G. J., Lansbury, P. T., and Caughey, B. (1994) *Nature* **370,** 471–474
38. Harper, J. D., and Lansbury, P. T., Jr. (1997) *Annu. Rev. Biochem.* **66,** 385–407
39. Manuelidis, L. (1998) *Proc. Natl. Acad. Sci. U. S. A.* **95,** 2520–2525
40. Bartz, J. C., Kramer, M. L., Sheehan, M. H., Hutter, J. A., Ayers, J. I., Bessen, R. A., and Kincaid, A. E. (2007) *J. Virol.* **81,** 689–697

Journal of General Virology (2009), 90, 261–268 DOI 10.1099/vir.0.004754-0

Alteration of the biological and biochemical characteristics of bovine spongiform encephalopathy prions during interspecies transmission in transgenic mice models

Takashi Yokoyama, Kentaro Masujin, Yoshifumi Iwamaru, Morikazu Imamura and Shirou Mohri

Prion Disease Research Center, National Institute of Animal Health, Tsukuba, Ibaraki 305-0856, Japan

Correspondence
T. Yokoyama
tyoko@affrc.go.jp

Received 9 June 2008
Accepted 27 August 2008

In the interspecies transmission of prions, the species barrier influences the susceptibility of the host. Bovine spongiform encephalopathy (BSE) prions affect a wide range of host species but do not affect hamsters. In order to study this species barrier, this study analysed the transmissibility of BSE prions to several lines of transgenic (Tg) mice, including those expressing mouse and hamster chimeric prion proteins (MH2M and MHM2 mice). BSE prions were transmitted to tga20, MHM2 and ICR mice, and the incubation period was approximately 400 days. Thus, these mice were classified as 'susceptible mice'. However, BSE prions were not transmitted to MH2M and TgHaNSE mice, and these mice were classified as 'resistant mice'. After the BSE prions were passaged once in wild-type mice, they could be transmitted to resistant mice. The characteristics of the accumulated abnormal isoform of PrP (PrP^{Sc}) in susceptible and resistant mice were determined using Western blotting. A BSE-like glycoform pattern of PrP^{Sc} was detected in all of the susceptible mice using two different antibodies that recognized either the N- or the C-terminal end of the 27–30 kDa protease-resistant fragment of PrP (PrP_{27-30}) as the epitope. In contrast, proteinase digestion followed by deglycosylation analysis showed that, in addition to PrP_{27-30}, truncated PrP^{Sc} fragments existed in resistant mice. These mixed PrP^{Sc} fragments may have resulted from the adaptation of resistant mice to BSE prions.

INTRODUCTION

Bovine spongiform encephalopathy (BSE) is a type of transmissible spongiform encephalopathy or prion disease (Prusiner, 1991). The host gene-encoded cellular isoform of prion protein (PrP^{C}) and the conversion of PrP^{C} to the abnormal isoform (PrP^{Sc}) is the central event in prion pathogenesis. PrP^{Sc} is the major component of the prion, if not the entire infectious agent. With interspecies transmission of prions, which means that the PrP^{Sc} in the inoculum has a different amino acid sequence to the PrP^{C} in the host, prolonged incubation periods and/or less efficient transmissibility have been observed, and this phenomenon is referred to as the 'species barrier' (Kimberlin, 1991). At the molecular level, species barriers can be explained, at least partly, by the dependence of PrP^{C} formation on the PrP amino acid sequence homology.

Surprisingly, BSE prions affect a wide range of host species. In nature, BSE is transmitted to cattle (Wells & Wilesmith, 1995), several zoo ruminants (Kirkwood & Cunningham, 1994) and wild and domestic cats (Wyatt *et al.*, 1990, 1991). Experimentally, BSE has been transmitted to mice (Fraser *et al.*, 1992), sheep, goats (Foster *et al.*, 1993), minks (Robinson *et al.*, 1994), marmosets (Baker *et al.*, 1998), macaques (Lasmézas *et al.*, 1996) and lemurs (Bons *et al.*, 1999). Furthermore, BSE has been transmitted to humans, in whom it causes variant Creutzfeldt–Jakob disease (vCJD) (Collinge *et al.*, 1996; Hill *et al.*, 1997). However, BSE prions are not transmitted to hamsters. Mice and hamsters are good models for analysing the mechanisms underlying the species barrier to BSE prions.

Transgenic (Tg) mice that express heterologous PrP genes are useful tools for analysis of the species barrier. Eight amino acid differences are present between the mouse and hamster proteinase K (PK)-resistant 27–30 kDa core fragment of PrP^{Sc} (PrP_{27-30}). Studies using Tg mice have shown that the sequence of PrP influences the interspecies transmission of prions between mice and hamsters (Scott *et al.*, 1989, 1993). Transmission studies using mouse and hamster chimeric PrP-expressing mice (MHM2 and MH2M, respectively) have shown that the tertiary structure of the interacting sites of PrP^{C} and PrP^{Sc} may depend partially on the side chains of one or more of the amino acids at positions 138, 154 and 169 (Scott *et al.*, 1993).

Furthermore, *in vitro* analysis has shown that residue 155 in hamsters (equivalent to residue 154 in the mouse sequence) is necessary for the efficient formation of PK-resistant PrP (Priola *et al.*, 2001). However, the precise mechanism underlying the species barrier has not yet been elucidated.

Here, we examined the species barrier to BSE prions using a chimeric PrP expression mouse model. MHM2 and MH2M mice (Scott *et al.*, 1993) were inoculated intracerebrally with BSE prions. We found that aa 131–188 of PrP also contributed to the species barrier against BSE prions in hamsters. Following passage in mice, this barrier disappeared and the biological characteristics of the BSE prions changed: these prions could then affect MH2M mice. We analysed the characteristics of the accumulated PrP^{Sc} in the brains of these Tg mice. Accumulation of another truncated PrP^{Sc} was observed in MH2M mice, which were resistant to BSE prions of the primary passage.

METHODS

Animals and prions. Three-week-old female ICR mice (SLC) were purchased and used as wild-type mice. Tg mice that expressed mouse and hamster chimeric PrP (MH2M and MHM2, respectively) were provided by Dr S. B. Prusiner (Scott *et al.*, 1993). A comparison of the PrP amino acid sequence of these Tg mice is shown in Table 1. Amino acid substitutions of L108M and V111M are present in MHM2 mice. In addition to these amino acid substitutions, three other substitutions (I138M, Y154N and S169N) are present in MH2M mice. MHM2 and MH2M mice are susceptible to mouse-passaged and hamster-passaged prions, respectively (Scott *et al.*, 1993; Yokoyama *et al.*, 2007b) and these mice express different glycoforms of PrP^{C} (Yokoyama *et al.*, 2007b). tga20 mice, which overexpress mouse PrP (Fischer *et al.*, 1996), were purchased from the European Mutant Mice Association (EMMA). TgHaNSE mice, which overexpress hamster PrP in their neurons, were provided by Dr B. Chesebro (Race *et al.*, 1995). TgBoPrP mice, which overexpress cattle PrP, were provided by Dr S. B. Prusiner (Scott *et al.*, 1997). The susceptibility of TgBoPrP mice to BSE has been confirmed previously (Yokoyama *et al.*, 2007a). All of the Tg mice were maintained by crossing with $PrP^{0/0}$ mice (Yokoyama *et al.*, 2001) as a PrP-null background. Brain samples of BSE-affected cattle in Japan were used for the transmission study. Mouse-passaged BSE prions (Hayashi *et al.*, 2005) were also used, along with the mouse-adapted scrapie Obihiro strain and hamster-adapted scrapie Sc237 strain (Yokoyama *et al.*, 1995).

Incubation time assay. BSE and scrapie prions were transmitted to Tg mice as described previously (Yokoyama *et al.*, 1995). An outline of the transmission studies is shown in Fig. 1. Brain homogenates were prepared using a Multi-Beads Shocker (Yasui Kikai). Mice were inoculated with 20 µl 10 % homogenate (w/v) in sterile PBS. After inoculation, the clinical status of the mice was monitored daily to assess the onset of neurological signs. Diseased mice were sacrificed and subjected to examination for PrP^{Sc}, as described previously (Yokoyama *et al.*, 2001).

Western blotting. PrP^{Sc} was extracted from the mice brains according to a previously described method (Yokoyama *et al.*, 2001). The brain tissue (brain stem) was homogenized in buffer containing 100 mM NaCl and 50 mM Tris/HCl (pH 7.6). The homogenate was mixed with an equal volume of detergent buffer containing 4 % Zwittergent 3-14, 1 % Sarkosyl, 100 mM NaCl and 50 mM Tris/HCl (pH 7.6), and then incubated with 40 µg PK ml^{-1} at 37 °C for 30 min. PK digestion was terminated with 2 mM 4-(2-aminoethyl)-benzenesulfonyl fluoride hydrochloride (Pefablock; Roche Diagnostics). The sample was mixed with an equal volume of a gel-loading buffer containing 2 % SDS and heated at 100 °C for 6 min. The samples were separated by 12 % SDS-PAGE and electrically blotted onto a PVDF membrane (Immobilon-P; Millipore). The blotted membrane was incubated with anti-PrP antibodies. Polyclonal antibody (pAb) B103 (Horiuchi *et al.*, 1995) and monoclonal antibodies (mAbs) 44B1 (Kim *et al.*, 2004), T2 (Hayashi *et al.*, 2005) and 3F4 (Signet Laboratories) were used as primary antibodies. These antibodies recognized different epitopes: one located at the N terminus of PK-digested PrP^{Sc} (pAb B103 and mAb 3F4) and the others located at the C terminus of the globular domain of PrP^{Sc} (mAbs T2 and 44B1). mAbs T2 and 44B1 recognized the epitope located at aa 132–230 and 155–231 of PrP, respectively. Signals were detected using a chemiluminescent substrate (SuperSignal; Pierce Biotechnology).

Band profile of PK-digested PrP^{Sc}. For band analysis, the relative quantities of the three PrP^{Sc} bands were measured using Fluorochem software (Alpha-Innotech) after background subtraction. For band profile analysis, only samples within the linear range, i.e. those with unsaturated signal intensities, were used. All values were calculated as the mean ± SD of at least three independent determinations.

Table 1. Comparison of the PrP amino acid sequences of MHM2 and MH2M mice

The PrP amino acid sequence at residues 108, 111, 138, 154 and 169 is shown. Residue numbers correspond to those in murine PrP (Westaway *et al.*, 1987).

Species	PrP amino acid				
	108	111	138	154	169
Mouse	L	V	I	Y	S
MHM2	M	M	I	Y	S
MH2M	M	M	L	N	N
Hamster	M	M	L	N	N
Cattle	M	V	I	H	S

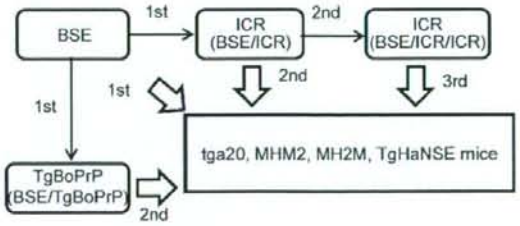

Fig. 1. Summary of the transmission experiment. BSE prions or mouse-passaged BSE prions (BSE/ICR or BSE/ICR/ICR) were inoculated intracerebrally into ICR, tga20, MHM2, MH2M and TgHaNSE mice. The clinical status of the mice was monitored. TgBoPrP-passaged BSE prions (BSE/TgBoPrP) were also inoculated into the same set of mice. 1st, 2nd and 3rd indicates the passage history of the BSE prions.

Peptide *N*-glycosidase F digestion. The PK-digested brain samples (10% brain homogenate; NP-40 lysis buffer) were denatured in glycoprotein-denaturing buffer (0.5% SDS, 1% β-mercaptoethanol; New England Biolabs) at 100 °C for 10 min prior to incubation with peptide *N*-glycosidase F (PNGase F; New England Biolabs) and G7 reaction buffer (50 mM $NaPO_4$; New England Biolabs) at 37 °C for 2–4 h. The reaction was terminated by SDS denaturation.

RESULTS

Transmission of BSE prions in cattle brain to Tg mice

BSE prions in cattle brain were transmitted to wild-type (ICR), MHM2 and tga20 mice, and the incubation period was approximately 400 days. However, 600 days after inoculation, MH2M and TgHaNSE mice showed no clinical signs of infection, and no PrP^{Sc} was detected in the sacrificed MH2M and TgHaNSE mice. Thus, MH2M and TgHaNSE mice were resistant to the BSE prions from cattle brains (Table 2). Depending on the transmissibility of the BSE prions from cattle brains, these mice were classified as 'susceptible mice' (ICR, MHM2 and tga20 mice) and 'resistant mice' (MH2M and TgHaNSE mice). The different susceptibilities of MH2M and MHM2 mice to BSE prions suggested that the species barrier of hamsters against BSE prions is due to region aa 131–188 of PrP, which included three amino acid substitutions (aa 138, 154 and 169) (Table 1). In this study, the incubation period in BSE-affected tga20 mice (456.5 days) was longer than that in wild-type mice (408.6 days) (Table 2). Overexpression of heterologous PrP did not shorten the incubation period in the primary interspecies transmission experiment. The shorter incubation period in the Tg mice infected with either mouse- or hamster-adapted scrapie prions is also shown in Table 2. The incubation periods of mouse-adapted scrapie prions were shorter than those of hamster-adapted scrapie prions in the susceptible mice (ICR, MHM2 and tga20) and vice versa in the resistant mice (MH2M and TgHaNSE).

Transmissibility of mouse-passaged BSE prions

Next, the transmissibility of wild-type mouse-passaged BSE prions was examined using the same set of Tg mice as in the primary transmission experiment. The MH2M and TgHaNSE mice showed clinical signs 212.8 and 153.1 days after inoculation, respectively (Table 2). The presence of PrP^{Sc} in their brains also supported the transmissibility (Fig. 2b). Mouse-passaged BSE prions were transmissible to all of the examined mice, including the MH2M and TgHaNSE mice. Subsequently, the mouse-passaged BSE prions were also used to challenge the same set of mice. In the wild-type mice, the incubation period of BSE prions was shortened, depending on the passage history. These Tg mice were also inoculated with secondary mouse-passaged BSE prions in order to monitor the transition of biological characteristics. Although the incubation periods in MH2M and TgHaNSE mice in the second and third passages were unstable, MHM2 and tga20 mice showed similar incubation periods in both the second and third passages (Table 2). The susceptibility of Tg mice to mouse-passaged BSE prions differed from that to the original BSE prions. Moreover, mouse-passaged BSE prions showed different biological characteristics from those in the first passage.

Transmissibility of TgBoPrP-passaged BSE prions

We examined the host range of TgBoPrP-passaged BSE prions. BSE prions were inoculated into TgBoPrP mice and the diseased mice brain homogenate was inoculated intracerebrally into TgBoPrP, ICR, tga20, MHM2, MH2M and TgHaNSE mice. The transmissibility of TgBoPrP-passaged BSE (BSE/TgBoPrP) resembled that of BSE: the prions of both could be transmitted to ICR, TgBoPrP, MHM2 and tga20 mice but not to MH2M and TgHaNSE mice (Table 2). The incubation periods of TgBoPrP mice inoculated with BSE and BSE/TgBoPrP were similar. In contrast, those of ICR, tga20 and MHM2 mice

Table 2. Incubation periods of BSE prions in Tg mice

Brain homogenate (10%) was inoculated intracerebrally into five to seven mice. PrP^{Sc} was detected in all of the diseased mice. Results are shown as mean ± SD (days). The passage number of the inoculum is indicated in parentheses. ND, Not done.

Mice	Inoculum				Incubation period with mouse or hamster adapted prions	
	BSE (1st)	BSE/ICR (2nd)	BSE/ICR/ICR (3rd)	BSE/TgBoPrP (2nd)*	Obihiro/ICR	Sc237/Hamster
ICR	408.6 ± 28.2	196.8 ± 8.4	173.6 ± 7.9	347.2 ± 55.9	150.0 ± 2.5	>600†
MHM2	399.6 ± 56.7	127.7 ± 4.3	123.8 ± 2.4	222.0 ± 20.7	159.1 ± 7.4	420.5 ± 17.2
MH2M	>600†	212.8 ± 16.4	185.0 ± 3.4	>600†	187.4 ± 7.5	102.3 ± 3.6
Tga20	456.5 ± 49.5	122.3 ± 11.3	123.6 ± 2.4	348.6 ± 57.9	78.3 ± 2.9	ND
TgHaNSE	>600†	153.1 ± 1.1	164.4 ± 6.8	>600†	ND	47.2 ± 3.6
TgBoPrP	223.5 ± 13.5				ND	ND

*Diseased brain homogenate from the first passage of TgBoPrP-passaged BSE (BSE/TgBoPrP) was used to infect mice.
†Mice and hamsters showed no clinical signs 600 days after inoculation. PrP^{Sc} was negative in these rodent brains.

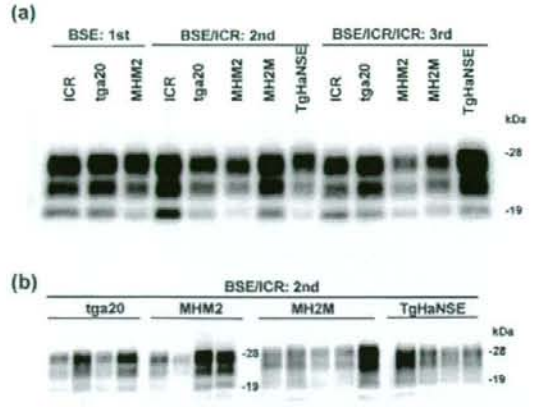

Fig. 2. Western blot analysis of PrP^{Sc} in Tg mice. (a) PrP^{Sc} in mouse brains were detected by pAb B103. BSE, BSE/ICR and BSE/ICR/ICR indicate the inoculum used. (b) PrP^{Sc} in the twice-passaged mice was detected with mAb T2.

inoculated with BSE/TgBoPrP were shortened compared with inoculation with BSE. In particular, the incubation period in MHM2 mice was considerably shortened to 222.0 days (Table 2).

Molecular properties of PrP^{Sc} from BSE prion-infected Tg mice

All of the diseased mice harboured PrP^{Sc} in their brains. The typical three PrP^{Sc} bands were detected with pAb B103 analysis (Fig. 2a). Glycoform analysis revealed dominant high-molecular-mass (di-glycosylated) PrP^{Sc} in all of the Tg mice (Fig. 3a). In contrast, a different banding pattern was observed with the use of antibodies against the globular domain of PrP^{Sc} (mAbs T2 and 44B1) from the mouse-passaged-BSE-affected MH2M and TgHaNSE mice (second passage) (Fig. 2b). The PrP^{Sc} bands from the BSE/ICR-passaged MH2M and TgHaNSE mice appeared smeared between the high- and medium-molecular-mass bands, with a long exposure period required for detection. The amount of high-molecular-mass PrP^{Sc} was decreased, whilst the amounts of medium- and low-molecular-mass PrP^{Sc} were increased (Fig. 3b). The different PrP^{Sc} band patterns were not obtained using pAb B103 and mAb T2 in other mice (ICR, tga20 and MHM2) (Figs 2b and 3b). Furthermore, BSE/ICR/ICR-passaged ICR, tga20, MH2M and TgHaNSE mice (third passage) showed different PrP^{Sc} band ratios in the mAb T2 analysis (Fig. 3b) and mAb 44B1 analysis (data not shown).

Western blot analysis showed different banding patterns for PrP^{Sc} in BSE-affected MH2M and TgHaNSE mice. The molecular mass of PK-digested PrP^{Sc} was analysed. After PNGase F digestion, the core of the PK-digested PrP^{Sc} detected using pAb B103 was similar among all of the BSE-

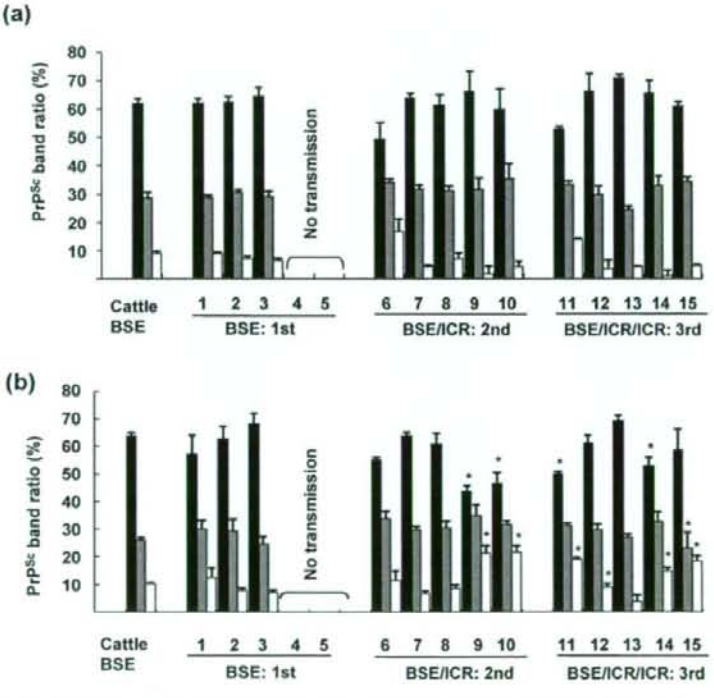

Fig. 3. PrP^{Sc} band patterns in Tg mice detected using pAb B103 (a) and mAb T2 (b). Data are shown as means ± SD (n=4). Lanes: 1, 6 and 11, ICR mice; 2, 7 and 12, tga20 mice; 3, 8 and 13, MHM2 mice; 4, 9 and 14, MH2M mice; 5, 10 and 15, TgHaNSE mice. Filled columns, high-molecular-mass PrP^{Sc}; shaded columns, medium-molecular-mass PrP^{Sc}; open columns, low-molecular-mass PrP^{Sc}. * indicates a significantly different band ratio observed in (b) compared with (a) (P<0.05). The inocula are indicated as BSE, BSE/ICR and BSE/ICR/ICR. Cattle BSE, band pattern of PrP^{Sc} from the BSE cattle brain.

affected Tg mice. In contrast, the core detected using mAb 44B1 was different in the MH2M mice (Fig. 4a). The cores in the ICR, tga20 and MHM2 mice converged to one band. However, those in the MH2M mice converged to two bands, which were about 19 and 17.5 kDa, respectively (Fig. 4a). The core fragment of PrP^{Sc} from MHM2 and MH2M mice passaged two and three times was analysed. As shown in Fig. 4(b), a distinct additional band was observed in MH2M mice, but not in MHM2 mice, regardless of the passage history. A similar result was also obtained by mAb T2 analysis (data not shown).

Characteristics of PrP^{Sc} in TgBoPrP-passaged BSE-affected mice

The glycoform pattern and molecular mass of PrP^{Sc} accumulated in the brains of BSE- and BSE/TgBoPrP-inoculated mice were analysed. The band pattern of PrP^{Sc} in BSE/TgBoPrP-affected mice resembled that of PrP^{Sc} in BSE-affected mice, as determined using mAb 44B1 (Fig. 5).

DISCUSSION

It is known that BSE prions can be transmitted to a wide range of species. The occurrence of vCJD has highlighted the interspecies transmission of BSE. No successful transmission of BSE prions was observed in MH2M and

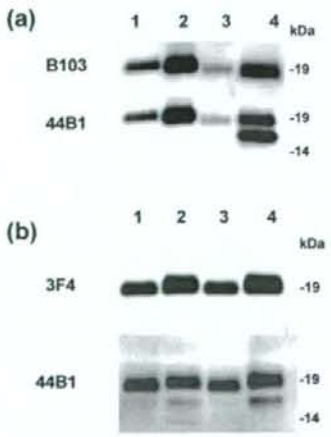

Fig. 4. Analysis of PNGase F-treated PrP^{Sc}. PK-digested PrP^{Sc} was subjected to PNGase F treatment. (a) The core fragment of PrP^{Sc} was detected with pAb B103 (upper panel) and mAb 44B1 (lower panel). Lanes: 1, scrapie Obihiro strain-affected ICR mice; 2, BSE-affected ICR mice; 3, BSE-affected tga20 mice; 4, BSE/ICR-affected MH2M mice. (b) The core fragment of PrP^{Sc} was detected with mAb 3F4 (upper panel) and mAb 44B1 (lower panel). Lanes: 1, BSE/ICR-affected MHM2 mice; 2, BSE/ICR-affected MH2M mice; 3, BSE/ICR/ICR-affected MHM2 mice; 4, BSE/ICR/ICR-affected MH2M mice.

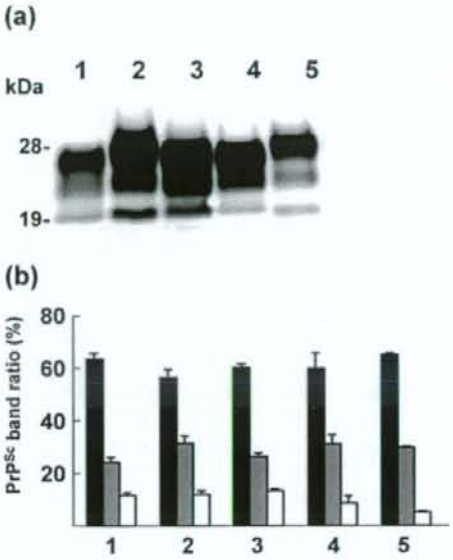

Fig. 5. Western blot analysis of PrP^{Sc} in TgBoPrP-passaged BSE. (a) Western blot results. Lanes: 1, BSE-affected TgBoPrP mice (first passage); 2, BSE/TgBoPrP-affected ICR mice; 3, BSE/TgBoPrP-affected TgBoPrP mice; 4, BSE/TgBoPrP-affected MHM2 mice; and 5, BSE/TgBoPrP-affected tga20 mice. PrP^{Sc} was detected with mAb 44B1. (b) Banding patterns of PrP^{Sc} in Tg mice. The brain samples of Tg mice inoculated intracerebrally with BSE/TgBoPrP were analysed. The numbers indicate the same mouse as in (a). Filled columns, high-molecular-mass PrP^{Sc}; shaded columns, medium-molecular-mass PrP^{Sc}; open columns, low-molecular-mass PrP^{Sc}. PrP^{Sc} was detected with mAb 44B1.

TgHaNSE mice in the primary passage, so they were classified as resistant mice. In contrast, tga20, MHM2 and wild-type mice were susceptible to BSE prions (Table 2). The PrP amino acid sequence comparison between MH2M and MHM2 mice showed that three amino acid substitutions located at aa 131–188 of PrP might contribute to the species barrier against BSE in hamsters. Residue 154 determines the efficiency of PrP^{Sc} formation induced by hamster PrP^{C} and is associated with the species barrier between mice and hamsters (Priola *et al.*, 2001). There was no commonality among these three amino acid substitutions with regard to the cattle PrP sequence (Table 1). It is well known that susceptibility to scrapie in sheep is determined by residue 171 of ovine PrP (Hunter *et al.*, 1997), and that codon 129 in humans is associated with susceptibility to vCJD (Hill *et al.*, 1997). Residue 142 in goat PrP is associated with resistance to both scrapie and BSE (Goldmann *et al.*, 1996). The barrier to interspecies prion transmission can be enhanced by mismatches in key amino acid residues, but the most influential residues are not always the same in every species (Moore *et al.*, 2005).

Interestingly, BSE prions that were passaged once in wild-type mice could be transmitted to resistant mice. This implies that passage of BSE prions in different species alters their biological characteristics. It has been reported that the virulence of BSE prions is enhanced on crossing the species barrier (Espinosa *et al.*, 2007). We also confirmed that the range of host species susceptible to prion strains may not be constant; rather, it may easily change via interspecies transmission. This means that the risk analysis of newly emerging prion diseases should be carefully considered.

The incubation periods of BSE prions in wild-type mice were decreased depending on the number of passages (Table 2), and complete adaptation of BSE prions to wild-type mice required four passages. The shortened incubation periods were approximately 150 days long (data not shown). In contrast, the incubation periods in tga20 mice in the second (122.3 days) and third (123.6 days) mouse passages of BSE prions were similar (Table 2). MHM2 mice also showed similar incubation periods between BSE/ICR (second passage) and BSE/ICR/ICR (third passage) mice (Table 2). This result indicated that overexpression of PrP^{C} during the serial passages may overcome the barrier to prion adaptation. However, no significant difference was found among the incubation periods for ICR, tga20 and MHM2 mice in the first passage (Table 2). This suggested that the overexpression of heterologous PrP could not overcome the barrier to interspecies transmission in the primary passage experiment. The prion adaptation process for overcoming the species barrier might comprise several steps – one of these is associated with PrP^{C}, whilst the other is not. Differences in the primary PrP sequence constitute part of the species barrier and these are not affected by heterologous PrP^{C} overexpression, which overcomes the other element of the barrier.

To confirm the existence of related host factors other than PrP^{C}, the biological characteristics of BSE/TgBoPrP prions were analysed. The susceptibility of Tg mice to BSE/TgBoPrP was similar to that to BSE prions. However, the incubation period in BSE/TgBoPrP-inoculated MHM2 mice was significantly shortened and was equal to that in TgBoPrP mice (222 days) (Table 2). The incubation time assay using a set of Tg mice could be utilized for monitoring the alterations in prion characteristics. Our result may indicate that the biological characteristics of BSE prions are influenced by unidentified characteristics other than those of the host PrP^{C}, or that the PrP^{C} of MHM2 mice conforms most closely to cattle PrP^{C} in Tg mice and that this similarity is related to the conversion efficiency of PrP^{Sc} from BSE prions. Further studies should be conducted to address these issues.

The PrP^{Sc} glycoform is utilized for prion strain classification (Collinge *et al.*, 1996). PrP^{Sc} in all of the Tg mice showed a BSE-like glycoform pattern with an antibody (pAb B103) that recognized the N-terminal end of PrP_{27-30} as the epitope (Fig. 2a). PrP^{Sc} in the susceptible mice also showed a BSE-like glycoform pattern with a different antibody (mAb T2) that recognized the C-terminal end of PrP_{27-30} (Fig. 3b). In contrast, the use of mAb T2 revealed a different PrP^{Sc} band pattern in MH2M and TgHaNSE mice at the second passage. Deglycosylation analysis showed that this banding pattern was not derived from different glycoform modifications, but demonstrated the presence of truncated PrP fragments in MH2M mice (Fig. 4). Our results showed the accumulation of another PK-resistant PrP^{Sc} fragment in the resistant mice. The N-terminal end of PK-digested PrP^{Sc} of mouse-passaged BSE prions converged to N96 in the susceptible mice (Hayashi *et al.*, 2005). At the third passage, mAb T2 analysis of ICR and tga20 mice also showed different band patterns. However, the PrP^{Sc} of these mice converged to one band with PNGase F treatment (data not shown). The different PrP^{Sc} band patterns of ICR and tga20 mice at the third passage were caused by different glycoform modifications and were not due to the presence of mixed PrP^{Sc} bands.

It has been reported that the shift in the size of PK-digested PrP^{Sc} occurs during the cross-sequence transmission of sporadic CJD to Tg mice (Kobayashi *et al.*, 2007), mice inoculated with vCJD prions (Hill *et al.*, 1997) and mice inoculated with hamster Sc237 prions (Hill *et al.*, 2000). The altered size of the PrP^{Sc} of mouse-passaged Sc237 reverted to its original size following transmission to hamsters (Hill *et al.*, 2000). In this study, we detected other truncated PrP^{Sc} fragments in the BSE prion-infected resistant animal. The adaptation to the new host PrP^{C} and/or selection of a PrP^{Sc} subpopulation from heterogeneous PrP^{Sc} may result in the emergence of a new prion strain.

Recently, the occurrence of atypical BSE with different PrP^{Sc} characteristics has been reported (Biacabe *et al.*, 2004; Casalone *et al.*, 2004; Yamakawa *et al.*, 2003). Atypical BSE has been classified into L type and H type according to the molecular mass of the unglycosylated PrP^{Sc} (Buschmann *et al.*, 2006). The altered N-terminal end of PK-digested PrP^{Sc} may influence the biological phenotype of atypical BSE. The appearance of two non-glycosylated fragments has been reported in H-type BSE, which is thought to indicate the strain-dependent nature of this molecular phenomenon (Jacobs *et al.*, 2007). The truncated PrP^{Sc} detected in resistant mice may be a good model to generate different conformations of PrP^{Sc}. The pathogenicity of truncated PrP^{Sc} fragments should be studied to elucidate the origin of different PrP^{Sc} phenotypes.

ACKNOWLEDGEMENTS

We thank Dr Motohiro Horiuchi for providing mAb 44B1 and pAb B103. We would also like to thank Dr Morikazu Shinagawa for his encouragement; Ms Hiroko K. Hayashi, Kimi Shimada, Naoko Tabeta and Shuko Kodani for their technical assistance; Ms Junko Yamada for her general assistance; and Ms Che Jing Zh and the animal laboratory staff at the National Institute of Animal Health for maintaining the mouse colony. This study was supported in part by a

grant for BSE research from the Ministry of Health, Welfare and Labour of Japan; a Grant-in-Aid from the Bovine Spongiform Encephalopathy Control Project of the Ministry of Agriculture, Forestry and Fisheries of Japan; and a grant from the Special Coordination Funds for Strategic Cooperation to Control Emerging and Re-emerging Infections from the Ministry of Education, Culture, Sports, Science and Technology, Japan.

REFERENCES

Baker, H. F., Ridley, R. M., Wells, G. A. & Ironside, J. W. (1998). Prion protein immunohistochemical staining in the brains of monkeys with transmissible spongiform encephalopathy. *Neuropathol Appl Neurobiol* **24**, 476–486.

Biacabe, A. G., Laplanche, J. L., Ryder, S. & Baron, T. (2004). Distinct molecular phenotypes in bovine prion diseases. *EMBO Rep* **5**, 110–114.

Bons, N., Mestre-Frances, N., Belli, P., Cathala, F., Gajdusek, D. C. & Brown, P. (1999). Natural and experimental oral infection of nonhuman primates by bovine spongiform encephalopathy agents. *Proc Natl Acad Sci U S A* **96**, 4046–4051.

Buschmann, A., Gretzschel, A., Biacabe, A. G., Schiebel, K., Corona, C., Hoffmann, C., Eiden, M., Baron, T., Casalone, C. & Groschup, M. H. (2006). Atypical BSE in Germany – proof of transmissibility and biochemical characterization. *Vet Microbiol* **117**, 103–116.

Casalone, C., Zanusso, G., Acutis, P., Ferrari, S., Capucci, L., Tagliavini, F., Monaco, S. & Caramelli, M. (2004). Identification of a second bovine amyloidotic spongiform encephalopathy: molecular similarities with sporadic Creutzfeldt–Jakob disease. *Proc Natl Acad Sci U S A* **101**, 3065–3070.

Collinge, J., Sidle, K. C. L., Meads, J., Ironside, J. & Hill, A. F. (1996). Molecular analysis of prion strain variation and the aetiology of 'new variant' CJD. *Nature* **383**, 685–690.

Espinosa, J. C., Andréoletti, O., Castilla, J., Herva, M. E., Morales, M., Alamillo, E., San-Segundo, F. D., Lacroux, C., Lugan, S. & other authors (2007). Sheep-passaged bovine spongiform encephalopathy agent exhibits altered pathobiological properties in bovine-PrP transgenic mice. *J Virol* **81**, 835–843.

Fischer, M., Rülicke, T., Raeber, A., Sailer, A., Moser, M., Oesch, B., Brandner, S., Aguzzi, A. & Weissmann, C. (1996). Prion protein (PrP) with amino-proximal deletions restoring susceptibility of PrP knockout mice to scrapie. *EMBO J* **15**, 1255–1264.

Foster, J. D., Hope, J. & Fraser, H. (1993). Transmission of bovine spongiform encephalopathy to sheep and goats. *Vet Rec* **133**, 339–341.

Fraser, H., Bruce, M. E., Chree, A., McConnell, I. & Wells, G. A. H. (1992). Transmission of bovine spongiform encephalopathy and scrapie to mice. *J Gen Virol* **73**, 1891–1897.

Goldmann, W., Martin, T., Foster, J., Hughes, S., Smith, G., Hughes, K., Dawson, M. & Hunter, N. (1996). Novel polymorphisms in the caprine PrP gene: a codon 142 mutation associated with scrapie incubation period. *J Gen Virol* **77**, 2885–2891.

Hayashi, H. K., Yokoyama, T., Takata, M., Iwamaru, Y., Imamura, M., Ushiki, Y. K. & Shinagawa, M. (2005). The N-terminal cleavage site of PrP^{Sc} from BSE differs from that of PrP^{Sc} from scrapie. *Biochem Biophys Res Commun* **328**, 1024–1027.

Hill, A. F., Desbruslais, M., Joiner, S., Sidle, K. C. L., Gowland, I., Collinge, J., Doey, L. J. & Lantos, P. (1997). The same prion strain causes vCJD and BSE. *Nature* **389**, 448–450.

Hill, A. F., Joiner, S., Linehan, J., Desbruslais, M., Lantos, P. L. & Collinge, J. (2000). Species-barrier-independent prion replication in apparently resistant species. *Proc Natl Acad Sci U S A* **97**, 10248–10253.

Horiuchi, M., Yamazaki, N., Ikeda, T., Ishiguro, N. & Shinagawa, M. (1995). A cellular form of prion protein (PrP^{C}) exists in many non-neuronal tissues of sheep. *J Gen Virol* **76**, 2583–2587.

Hunter, N., Moore, L., Hosie, B. D., Dingwall, W. S. & Greig, A. (1997). Association between natural scrapie and PrP genotype in a flock of Suffolk sheep in Scotland. *Vet Rec* **140**, 59–63.

Jacobs, J. G., Langeveld, J. P. M., Biacabe, A. G., Acutis, P. L., Polak, M. P., Gavier-Widen, D., Buschmann, A., Caramelli, M., Casalone, C. & other authors (2007). Molecular discrimination of atypical bovine spongiform encephalopathy strains from a geographical region spanning a wide area in Europe. *J Clin Microbiol* **45**, 1821–1829.

Kim, C. L., Umetani, A., Matsui, T., Ishiguro, N., Shinagawa, M. & Horiuchi, M. (2004). Antigenic characterization of an abnormal isoform of prion protein using a new diverse panel of monoclonal antibodies. *Virology* **320**, 40–51.

Kimberlin, R. H. (1991). Agent host interactions and pathogenesis. In *Sub-acute Spongiform Encephalopathies*, pp. 137–147. Edited by R. Bradley, M. Savey & B. Marchant. Dordrecht: Kluwer Academic Publishers.

Kirkwood, J. K. & Cunningham, A. A. (1994). Epidemiological observations on spongiform encephalopathies in captive wild animals in the British Isles. *Vet Rec* **135**, 296–303.

Kobayashi, A., Asano, M., Mohri, S. & Kitamoto, T. (2007). Cross-sequence transmission of sporadic Creutzfeldt–Jakob disease creates a new prion strain. *J Biol Chem* **282**, 30022–30028.

Lasmézas, C. I., Deslys, J. P., Demaimay, R., Adjou, K. T., Lamoury, F., Dormont, D., Robain, O., Ironside, J. & Hauw, J. J. (1996). BSE transmission to macaques. *Nature* **381**, 743–744.

Moore, R. A., Vorberg, I. & Priola, S. A. (2005). Species barriers in prion diseases – brief review. *Arch Virol Suppl* **19**, 187–202.

Priola, S. A., Chabry, J. & Chan, K. (2001). Efficient conversion of normal prion protein (PrP) by abnormal hamster PrP is determined by homology at amino acid residue 155. *J Virol* **75**, 4673–4680.

Prusiner, S. B. (1991). Molecular biology of prion diseases. *Science* **252**, 1515–1522.

Race, R. E., Priola, S. A., Bessen, R. A., Ernst, D., Dockter, J., Rall, G. F., Mucke, L., Chesebro, B. & Oldstone, M. B. (1995). Neuron-specific expression of a hamster prion protein minigene in transgenic mice induces susceptibility to hamster scrapie agent. *Neuron* **15**, 1183–1191.

Robinson, M. M., Hadlow, W. J., Huff, T. P., Wells, G. A. H., Dawson, M., Marsh, R. F. & Gorham, J. R. (1994). Experimental infection of mink with bovine spongiform encephalopathy. *J Gen Virol* **75**, 2151–2155.

Scott, M., Foster, D., Mirenda, C., Serban, D., Coufal, F., Wälchli, M., Torchia, M., Groth, D., Carlson, G. & other authors (1989). Transgenic mice expressing hamster prion protein produce species-specific scrapie infectivity and amyloid plaques. *Cell* **59**, 847–857.

Scott, M., Groth, D., Foster, D., Torchia, M., Yang, S. L., DeArmond, S. J. & Prusiner, S. B. (1993). Propagation of prions with artificial properties in transgenic mice expressing chimeric PrP genes. *Cell* **73**, 979–988.

Scott, M. R., Safar, J., Telling, G., Nguyen, O., Groth, D., Torchia, M., Koehler, R., Tremblay, P., Walther, D. & other authors (1997). Identification of a prion protein epitope modulating transmission of bovine spongiform encephalopathy prions to transgenic mice. *Proc Natl Acad Sci U S A* **94**, 14279–14284.

Wells, G. A. H. & Wilesmith, J. W. (1995). The neuropathology and epidemiology of bovine spongiform encephalopathy. *Brain Pathol* **5**, 91–103.

Westaway, D., Goodman, P. A., Mirenda, C. A., McKinley, M. P., Carlson, G. A. & Prusiner, S. B. (1987). Distinct prion proteins in short and long scrapie incubation period mice. *Cell* **51**, 651–662.

Wyatt, J. M., Pearson, G. R., Smerdon, T. N., Gruffydd-Jones, T. J. & Wells, G. A. H. (1990). Spongiform encephalopathy in cat. *Vet Rec* **126**, 513.

Wyatt, J. M., Pearson, G. R., Smerdon, T. N., Gruffydd-Jones, T. J., Wells, G. A. H. & Wilesmith, J. W. (1991). Naturally occurring scrapie-like spongiform encephalopathy in five domestic cats. *Vet Rec* **129**, 233–236.

Yamakawa, Y., Hagiwara, K., Nohtomi, K., Nakamura, Y., Nishijima, M., Higuchi, Y., Sato, Y., Sata, T. & The Expert Committee for BSE diagnosis, Ministry of Health, Labour and Welfare of Japan (2003). Atypical proteinase K-resistant prion protein (PrP^{res}) observed in an apparently healthy 23-month-old Holstein steer. *Jpn J Infect Dis* **56**, 221–222.

Yokoyama, T., Kimura, K., Tagawa, Y. & Yuasa, N. (1995). Preparation and characterization of antibodies against mouse prion protein (PrP) peptides. *Clin Diagn Lab Immunol* **2**, 172–176.

Yokoyama, T., Kimura, K. M., Ushiki, Y., Yamada, S., Morooka, A., Nakashiba, T., Sassa, T. & Itohara, S. (2001). *In vivo* conversion of cellular prion protein to pathogenic isoforms, as monitored by conformation-specific antibodies. *J Biol Chem* **276**, 11265–11271.

Yokoyama, T., Msujin, K., Yamakawa, Y., Sata, T., Murayama, Y., Shu, Y., Okada, H., Mohri, S. & Shinagawa, M. (2007a). Experimental transmission of two young and one suspended bovine spongiform encephalopathy (BSE) cases to bovinized transgenic mice. *Jpn J Infect Dis* **60**, 317–320.

Yokoyama, T., Shimada, K., Masujin, K., Iwamaru, Y., Imamura, M., Ushiki, Y. K., Kimura, K. M., Itohara, S. & Shinagawa, M. (2007b). Both host prion protein 131–188 subregion and prion strain characteristics regulate glycoform of PrP^{Sc}. *Arch Virol* **152**, 603–609.

Journal of Neurochemistry

JOURNAL OF NEUROCHEMISTRY | 2008 | 107 | 636–646

doi: 10.1111/j.1471-4159.2008.05628.x

Lactoferrin induces cell surface retention of prion protein and inhibits prion accumulation

Yoshifumi Iwamaru,* Yoshihisa Shimizu,* Morikazu Imamura,* Yuichi Murayama,* Ryo Endo,* Yuichi Tagawa,* Yuko Ushiki-Kaku,† Takato Takenouchi,‡ Hiroshi Kitani,‡ Shirou Mohri,* Takashi Yokoyama* and Hiroyuki Okada*

*Prion Disease Research Center, National Institute of Animal Health, Ibaraki, Japan

†Nippi Research Institute of Biomatrix, Ibaraki, Japan

‡Transgenic Animal Research Center, National Institute of Agrobiological Sciences, Ibaraki, Japan

Abstract

Prion diseases are fatal neurodegenerative disorders, and the conformational conversion of normal cellular prion protein (PrP^C) into its pathogenic, amyloidogenic isoform (PrP^{Sc}) is the essential event in the pathogenesis of these diseases. Lactoferrin (LF) is a cationic iron-binding glycoprotein belonging to the transferrin (TF) family, which accumulates in the amyloid deposits in the brain in neurodegenerative disorders, such as Alzheimer's disease and Pick's disease. In the present study, we have examined the effects of LF on PrP^{Sc} formation by using cell culture models. Bovine LF inhibited PrP^{Sc} accumulation in scrapie-infected cells in a time- and dose-dependent manner, whereas TF was not inhibitory. Bioassays of LF-treated cells demonstrated prolonged incubation periods compared with non-treated cells indicating a reduction of prion infectivity. LF mediated the cell surface retention of PrP^C by diminishing its internalization and was capable of interacting with PrP^C in addition to PrP^{Sc}. Furthermore, LF partially inhibited the formation of protease-resistant PrP as determined by the protein misfolding cyclic amplification assay. Our results suggest that LF has multifunctional antiprion activities.

Keywords: amyloid, lactoferrin, N2a cells, prion, PrP^C, PrP^{Sc}.

J. Neurochem. (2008) **107**, 636–646.

Prion diseases are fatal, transmissible and progressive neurodegenerative disorders, including Creutzfeldt-Jakob disease in humans, bovine spongiform encephalopathy in cattle, scrapie in sheep and goats and chronic wasting disease in deer. At a molecular level, prion diseases are characterized by accumulation of a pathological isoform (PrP^{Sc}) of the host-encoded cellular prion protein (PrP^C) that is most prominent in the neural tissue. PrP^{Sc}, which co-purifies with infectivity (Gabizon *et al.* 1988), seems to be the main component of the agent of prion diseases (Prusiner 1982), and has therefore been used generally as a surrogate marker for prion infection. PrP^{Sc} is derived from PrP^C by post-translational conformational conversion resulting in differences in structure and biochemical properties of PrP. While PrP^C has high α-helix content and is protease sensitive, PrP^{Sc} is largely composed of β-sheets (Caughey *et al.* 1991b; Pan *et al.* 1993), is highly detergent insoluble and partially resistant to proteolytic digestion. Although mechanisms underlying the conversion have not been fully elucidated, it has been proposed that PrP^{Sc} directly interacts with PrP^C and mediates a conformational conversion of PrP^C into PrP^{Sc} (Prusiner 1991). This process occurs either on the cell surface of the infected cells or along the endocytic pathway (Caughey and Raymond 1991; Caughey *et al.* 1991a; Borchelt *et al.* 1992).

Until date, many substances that inhibit prion propagation have been identified. These include polysulphated

Received May 12, 2008; revised manuscript received July 9, 2008; accepted August 1, 2008.

Address correspondence and reprint requests to Yoshifumi Iwamaru, Prion Disease Research Center, National Institute of Animal Health, Kannonndai 3-1-5, Tsukuba, Ibaraki 305-0856, Japan.

E-mail: gan@affrc.go.jp

Abbreviations used: BSA, bovine serum albumin; EGFP, enhanced green fluorescence protein; GAGs, sulphated glycosaminoglycans; HRP, horseradish peroxidase; LF, lactoferrin; LFB, lactoferricin B; LPR/LR, laminin receptor precursors/lamin receptors; LRP, low-density lipoprotein receptor –related protein; Mab, monoclonal antibody; MesNa, sodium 2-mercaptoethanesulfonate; PK, proteinase K; PMCA, protein misfolding cyclic amplification; PNGase F, N-Glycosidase F; PrP, prion protein; ScN2a, scrapie-infected neuroblastoma cells; TF, transferrin.

polyanions (Caughey and Raymond 1993), polyamines (Supattapone *et al.* 1999), tetrapyrroles (Caughey *et al.* 1998), polyene antibiotics (Pocchiari *et al.* 1987), tetracyclic antibiotics (Forloni *et al.* 2002) and tricyclic compounds (May *et al.* 2003). Persistently scrapie-infected neuroblastoma cells (ScN2a) have been frequently used to screen antiprion substances as well as to clarify their mechanisms. Several therapeutic substances that diminish the formation of PrP^{Sc} in ScN2a cells can prolong the incubation period of scrapie infection in mice models (Doh-ura *et al.* 2004). Therefore, cell culture models using ScN2a cells offer a potentially powerful approach to screen compounds for an antiprion therapeutic agent.

Lactoferrin (LF) is an iron-binding glycoprotein with a molecular mass of 80 kDa that is found in milk and other secretions such as tears and saliva. LF has numerous biological roles including iron metabolism, antimicrobial activities (Arnold *et al.* 1977; van der Strate *et al.* 2001) and immune modulation. Thus, it is believed that LF plays an important role in host defence mechanisms. LF immunoreactivity has been reported to be present in the pathologic brain lesions in several neurodegenerative disorders including Alzheimer's disease, Down syndrome, amyotrophic lateral sclerosis and Pick's disease (Kawamata *et al.* 1993; Leveugle *et al.* 1994) where LF was found in senile plaques, neurofibrillary tangles and Pick bodies. Although the precise roles and mechanisms of LF in amyloid deposition are unclear, LF expression increases in neurons and glia in patients with Alzheimer's disease (Kawamata *et al.* 1993). In addition, an increased expression of LF receptors on microvessels and neurons has been reported in Parkinson's disease (Faucheux *et al.* 1995), suggesting that transcytosis of LF may become more efficient under certain conditions, such as those seen in neurodegenerative diseases. LF suppresses the production of inflammatory cytokines such as interleukin-1 and tumor necrosis factor alpha produced in monocyte (Crouch *et al.* 1992). It is thus postulated that LF accumulation in amyloid deposits plays a neuroprotective role. Moreover, LF prevents some denatured/misfolded proteins from aggregating (Takase 1998). These properties make LF an interesting therapeutic candidate against prion.

In this report, we have examined the effects of LF on PrP^{Sc} accumulation in scrapie-infected N2a58 (ScN2a58) cells. LF inhibited PrP^{Sc} accumulation in cells in a time- and dose-dependent manner. Bioassays of LF-treated cells in *tga*20 mice showed that LF also diminished prion infectivity. Based on experiments with normal cells treated with LF, we demonstrated that LF retains PrP^{C} on the cell-surface by interfering with the PrP^{C} internalization process. Moreover, LF bound to both PrP^{C} and PrP^{Sc} and partially interfered the formation of protease-resistant PrP as determined by the protein misfolding cyclic amplification (PMCA) assay. These findings indicate that LF has multifunctional anti-prion activities.

Materials and methods

Reagents and antibodies

N-Glycosidase F (PNGase F) was obtained from New England Biolabs (Beverly, MA, USA). Bovine LF was purchased from Wako Pure Chemical (Osaka, Japan), and all the other reagents were purchased from Sigma–Aldrich (St. Louis, MO, USA) unless otherwise specified. LF and TF were dissolved in Hanks' balanced salt solution (HBSS) at a stock concentration of 50 mg/mL and filtered through a 0.22-μm Millipore filter. Horseradish peroxidase (HRP)-conjugated streptavidin was purchased from GE Healthcare (Buckinghamshire, UK). HRP-conjugated goat anti-mouse antibodies were obtained from Jackson ImmunoResearch (West Grove, PA, USA). Anti-glyceraldehyde-3-phosphate dehydrogenase (GAPDH) monoclonal antibody (Mab) was obtained from HyTest (Turku, Finland). Anti-PrP mAbs SAF32 and SAF61 were obtained from SPI Bio (Montigny le Bretonneux, France). The Mab, 43C5, specific for residues 163–169 of mouse PrP (Kim *et al.* 2004a) was kindly donated by Dr M. Horiuchi (Hokkaido University, Hokkaido, Japan). Anti-PrP Mabs 3H2, 4E10 and T2 (Iwamaru *et al.* 2007) were produced in our laboratory in PrP-deficient mice by immunisation with proteinase K (PK)-untreated PrP^{Sc} (3H2) or mouse recombinant PrP (4E10 and T2). Epitope mapping for identifying linear epitopes was performed by pepspot analysis (Yokoyama *et al.* 2001). The epitopes of 3H2 and 4E10 were located between the residues 35–53 and 147–158 of mouse PrP, respectively (data not shown). Mab T2 recognizes discontinuous epitopes of residues 132–156 of mouse PrP based on the immunoblot reactivity of recombinant PrP deletion mutant (data not shown).

Cell culture and inhibition assay of PrP^{Sc} accumulation

N2a58 cells (Nishida *et al.* 2000) were kindly provided by Dr N. Nishida (Nagasaki University, Nagasaki, Japan). N2a58 cells persistently infected with mouse-adapted scrapie Chandler prion (ScN2a58 cells) were cultured in Opti-MEM supplemented with 10% heat-inactivated fetal calf serum at 37°C with 5% CO_2 and split every 4–5 days at 1 : 10 dilution. To investigate the effect of LF and TF on the production of PrP^{Sc}, ScN2a58 cells were plated in six-well plates (1×10^5 cells/well) and allowed to adhere overnight. Cells were cultured in the presence (5–1000 μg) or absence of LF and TF. Cells were then grown without changing the media and PrP^{Sc} production was evaluated after 6–72 h. At the end of the treatment, cells were washed with phosphate-buffered saline (PBS) without calcium and magnesium [PBS(–)] and then detached with PBS(–) containing 5 mM EDTA. After counting cell numbers, cell suspensions were divided into fractions treated with or without PK. The collected cells were then lysed with ice-cold lysis buffer (2×10^6 cells/mL) containing 10 mM Tris–HCl (pH 7.5), 150 mM NaCl, 1 mM EDTA with 0.5% Triton X-100 and 0.5% sodium deoxycholate for 20 min on ice. After centrifugation at 10 000 *g* for 2 min, 500 μL of each supernatant was digested with 20 μg/mL PK for 30 min at 37°C and the remainder was left untreated.

Cell viability

Cytotoxicity of LF was determined using the WST-8 assay (Cell Counting Kit-8, Dojindo Lab, Kumamoto, Japan). ScN2a58 cells grown in wells of a 96-well plate for 24 h were incubated in the medium containing the appropriate concentration of LF and TF for

72 h prior to the WST-8 assay according to the manufacturer's instructions. Treatment with each substance was performed in triplicate. Percentage cell viability in cultures was calculated by reference to untreated cells incubated with WST-8 (100%).

Immunoblot analysis

Cell cultures were washed once with ice-cold PBS(−) and lysed with ice-cold lysis buffer (1×10^6 cells/mL) for 15 min. After removal of insoluble debris by centrifugation at 10 000 *g* for 2 min, the supernatants were separated into two tubes. Samples without PK digestion were supplemented with 4 mM Pefabloc (Roche Molecular Biochemicals, Mannheim, Germany), and reserved for GAPDH or PrP^C analyses. For the detection of PrP^{Sc}, samples were digested with 20 μg/mL PK for 30 min at 37°C, adjusted to 4 mM with respect to Pefabloc and then ultracentrifuged at 200 000 *g* for 1 h in a TLA 55 rotor (Beckman Coulter, Fullerton, CA, USA). The samples were solubilized in sample loading buffer prior to electrophoresis on 12% NOVEX pre-cast gels (Invitrogen, San Diego, CA, USA). For immunoblot analysis, proteins were electrotransferred onto polyvinylidene fluoride membranes. The blots were reacted with anti-PrP Mabs T2 or 4E10 conjugated with HRP and anti-GAPDH Mab (HyTest) and developed by Super Signal West Dura (Pierce, Rockford, IL, USA). For quantification of PrP^{Sc}, blots were imaged with FluorChem (Alpha Innotech, San Leandro, CA, USA) and analyzed with AlphaEaseFC image reader software (Alpha Innotech) according to the manufacturer's instructions.

Mouse bioassay

Murine PrP over-expressing mice (*tga20* mice) were used for bioassay. The infectivity associated with ScN2a58 cell cultures was assayed by intracerebral inoculation into *tga*20 mice. ScN2a58 cells were harvested for inoculation at serial passage 10 (total 40 days) in the presence or absence of 500 μg/mL LF. The cells were suspended in sterile PBS(−), freeze-thawed and sonicated before intracranial inoculation (5×10^5 cells/20 μL/mouse). After inoculation, the terminally ill mice were killed for immunoblot of the brain. The survival time of two groups was statistically analyzed using the unpaired *t*-test. All mice were kept in an air-conditioned room and fed on standard laboratory food pellets and water *ad libitum*. The present study was performed according to the Guideline for Animal Experiments of National Institute of Animal Health (Tsukuba, Japan).

Analysis of PrP internalization

PrP internalization analysis was carried out using a modified version of a previously published procedure (Schmidt *et al.* 1997). N2a58 cells were grown to confluence, serum starved for 2 h, surface biotinylated using 1 mg/mL Sulfo-NHS-SS-biotin (Pierce) in PBS (pH 8.0) for 15 min on ice and washed with 50 mM glycine in HBSS to quench free sulfo-NHS-SS biotin, followed by further washes with HBSS. The cells were shifted to 37°C in Opti-MEM for 0–15 min to allow internalization of the biotinylated molecules. Cells were incubated with ice-cold NT buffer (150 mM NaCl, 1 mM EDTA, 0.2% bovine serum albumin (BSA) and 20 mM Tris–HCl at pH 8.5) for 5 min followed by incubation of NT buffer containing 20 mM sodium 2-mercaptoethanesulfonate (MesNa; a small membrane-impermeant thiol-reducing reagent) two times for 30 min. Cells were rinsed extensively with HBSS and incubated in HBSS containing 20 mM iodoacetic acid for 15 min to inactivate residual MesNa. Control cells were treated identically except that MesNa was omitted. Cells were scraped with a disposable scraper (Sumitomo Bakelite, Tokyo, Japan) from the plates in 1 mL of ice-cold NP-40 buffer (Wako Pure Chemical Industries, Ltd., Osaka, Japan) (150 mM NaCl, 1 mM EDTA, 1% NP-40 and 10 mM Tris–HCl at pH 7.5) containing complete protease inhibitor (Roche) and lysed for 30 min on ice. After centrifugation at 15 000 *g* for 2 min, Dynabeads (sheep anti-mouse IgG; Invitrogen) pre-incubated with Mab 43C5 were added to the cleared cell lysates and incubated for 1 h at 4°C with constant rotation to immunoprecipitate PrP. After rinsing three times with ice-cold NP-40 buffer, the magnetic beads were further washed with the same buffer for 1 h at 4°C. Proteins were eluted in sample buffer at 100°C and analyzed by immunoblot.

Coupling to magnetic beads

Coupling was performed according to the manufacturer's instructions. In brief, 2 mg of BSA, LF or TF was diluted in 1 mL of coupling buffer (0.1 M borate at pH 9.5) and added to coupling buffer-washed to syl activated paramagnetic beads (Dynabeads M-280, Invitrogen). After incubation for 24 h at 37°C, the beads coupled with BSA, LF or TF were washed twice with PBS containing 0.5% (w/v) BSA, LF or TF for 5 min, respectively, and then incubated with blocking buffer (0.2 M Tris–HCl at pH 8.5 containing 1% BSA, LF or TF, respectively) for 4 h at 37°C.

Binding assay

Brains from healthy mice and Chandler scrapie-infected mice at the terminal stage of the disease were minced with a Biomasher (Nippi, Tokyo, Japan) and suspended in ice-cold NP-40 buffer (2% weight/volume). Cells were lysed with the same buffer (2.5×10^6 cells/mL) for 20 min on ice. After removal of insoluble debris by centrifugation at 10 000 *g* for 2 min, the supernatants were collected. The paramagnetic beads pre-copuled with BSA, LF or TF were added to the cleared supernatants and incubated for 1 h at 4°C with constant rotation. After rinsing three times with ice-cold NP-40 buffer, the magnetic beads were further washed with the same buffer for 12 h at 4°C. After treatment with or without 20 μg/mL PK for 30 min at 37°C, proteins were eluted in sample buffer at 100°C and analyzed by immunoblot.

Expression plasmid construction

The enhanced green fluorescence protein (EGFP)-PrP expression plasmid was constructed as described below. The signal peptide of mouse PrP (amino acids 1–22) was amplified by PCR using primers 5′-CCGCTAGCCTATCAGTCATCATGGCGAACCTTG-3′ and 5′-AAACCGGTAAGCAGAGGCCGSACATCAGTC-3′ with a mammalian expression plasmid containing full-length mouse PrP (amino acids 1–254) carrying the 3F4 epitope as a template. The PCR products were cloned into pGEM-T Easy (Promega, Madison, WI, USA) and the insert sequence was determined by nucleotide sequencing. The inserts excised by restriction enzymes (*Nhe*I and *Age*I) were cloned 5′ of EGFP in the pEGFP-C1 (Clontech, Mountain View, CA, USA) using the *Nhe*I and *Age*I sites (SP-GFP). The region encoding amino acids 23–254 was PCR amplified using primers 5′-CTCGAGGCAAAAAGCGGCCAAAGCCTG-3′ and 5′-GTCGACCTCATCCCACGATCAGGAAG-3′. The PCR products

were cloned into pGEM-T easy and sequenced. The inserts excised by *Xho*I and *Sal*I digestion were cloned 3′ of EGFP in the SP-GFP vector using *Xho*I and *Sal*I sites (EGFP-PrP).

Confocal imaging

Cells grown on a cover glass were transiently transfected with the EGFP-PrP construct using Transfectin reagent (BioRad, Hercules, CA, USA). One day after transfection, cells were incubated with LF for 24 h. After rinsing with HBSS, these cells were fixed with ice-cold 4% paraformaldehyde in PBS for 15 min and examined with a Zeiss LSM520 inverse laser scan microscope.

Flow cytometric analysis

Cells grown on 100-mm cell culture dishes were incubated with LF for 24 h. After rinsing with ice-cold HBSS, cells were harvested by pipetting. Two micrograms of several anti-PrP antibodies were pre-labeled using a Zenon R-Phycoerythrin Mouse IgG labeling kit (Invitrogen) according to the manufacturer's instructions. Cells were incubated for 30 min at 4°C with each Zenon-labeled antibody, washed twice in HBSS containing 1% BSA and analyzed with an EPICS XL SYSTEM II flow cytometer (Beckman Coulter). Fluorescence of 1.5×10^4 cells/antibodies was acquired and analyzed using Cellquest software to quantify the surface expression of PrP by calculating the mean fluorescence intensities.

PMCA assay

Brains from healthy mice and Chandler scrapie-infected mice at the terminal stage of the disease were minced with a Biomasher (Nippi) and suspended in conversion buffer. After removal of insoluble debris by centrifugation at 4500 *g* for 5 min, the supernatants were collected. The Chandler brain homogenate was diluted 1 : 1000 with healthy brain homogenate. Serial dilutions of LF and TF in HBSS were added to the brain homogenates to obtain final concentrations of 5, 50, 500 and 1000 μg/mL. The samples were incubated at 37°C with agitation for 30 min and subjected to a cycle of sonication every hour as described previously (Murayama *et al.* 2007).

Statistical analysis

Values in the figures are expressed as means ± SD. To determine the statistical significance, Student's *t*-test for unpaired data was applied as appropriate. A value of $p < 0.05$ was considered significant.

Results

Inhibition of PrP^{Sc} formation and prion replication in ScN2a58 cells by LF

To study the influence of LF on prion propagation, ScN2a58 cells were exposed to various concentrations of LF and were incubated for 3 days. As controls, cells were incubated with holo-transferrin (TF), since LF shares 59% identical amino acids with TF. Cells were then collected, and following PK digestion, the levels of PrP^{Sc} in the culture were determined. The levels of PrP^{Sc} in cells treated with LF were reduced in a concentration-dependent manner, compared with non-treated cells (Fig. 1a and b). Similar results were obtained in ScN2a cells treated with LF (data not shown). The 50% inhibitory concentration (IC_{50}) value of LF was 128.9 μg/mL (1.6 μM). In contrast, TF exposure did not produce a decrease in the PrP^{Sc} levels in ScN2a58 cells, suggesting that the LF-mediated reductive effect was not attributable to the protein content in the medium. We also examined the peptide lactoferricin B (LFB), derived from the N-terminal region of LF by acid-pepsin hydrolysis, however, LFB treatment did not exhibit a reduction in PrP^{Sc} in ScN2a58 cells (data not shown). No apparent cytotoxicity and visible change in cell morphology following the incubation with LF or TF were observed in the WST-8 assay (Fig. 1b). In addition, determinations of the total cell number and GAPDH level revealed no observable differences between treated and non-treated cells (data not shown).

Cells were incubated for 6, 12, 24, 36, 48, 60 and 72 h with 500 μg/mL of LF to evaluate the kinetics of inhibitory effect of LF on PrP^{Sc} accumulation. A significant reduction in the PrP^{Sc} levels was observed after 36 h of exposure (Fig. 1c).

To determine the effects of LF on prion replication, bioassays of ScN2a58 cells treated with or without LF were conducted. ScN2a58 cells were serially passaged up to 10 times (total 40 days) in the presence of 500 μg/mL of LF. The levels of PrP^{Sc} in ScN2a58 cells became undetectable after five passages in the presence of LF and remained undetectable after additional five passages of culture in the LF-containing medium (Fig. 1d). Inoculation of *tga20* mice ($n = 8$) with LF-treated ScN2a58 cells (10 passages with 500 μg/mL LF) resulted in a mean incubation period of 149 ± 6.9 days, which was significantly longer ($p < 0.01$) than that of 91 ± 0.8 days in *tga20* mice ($n = 6$) concomitantly inoculated with untreated ScN2a58 cells (Fig. 1e). The prolonged incubation period indicates the reduction of prion infectivity in LF-treated cells.

LF-mediated increase in the ratio of full-length PrP^{C} to total PrPC

The potent activity of LF in preventing prion replication in ScN2a58 cells led us to explore the mechanisms underlying this activity. To examine whether the PrP^{Sc} reduction effect of LF was mediated by the suppression of PrP^{C} levels, the PrP^{C} levels in N2a58 cells treated for 3 days with various concentrations of LF were ascertained. PrP^{C} undergoes proteolytic cleavage to produce C-terminal fragments mainly consisting of approximately 17 kDa, which is referred to as the C1 fragment (Harris *et al.* 1993; Chen *et al.* 1995). Thus, we defined 'total PrP^{C}' as uncleaved PrP^{C} (full-length PrP^{C}) plus C-terminal fragments. Cell lysates not treated with PK were subjected to immunoblot and the total PrP^{C} levels were determined (Fig. 2a). Although LF did not substantially affect the total PrP^{C} levels, the full-length PrP^{C} levels increased in a concentration-dependent manner. An increase in the full-length PrP^{C} levels was further confirmed by immunoblot using Mab 3H2, which detects epitopes between

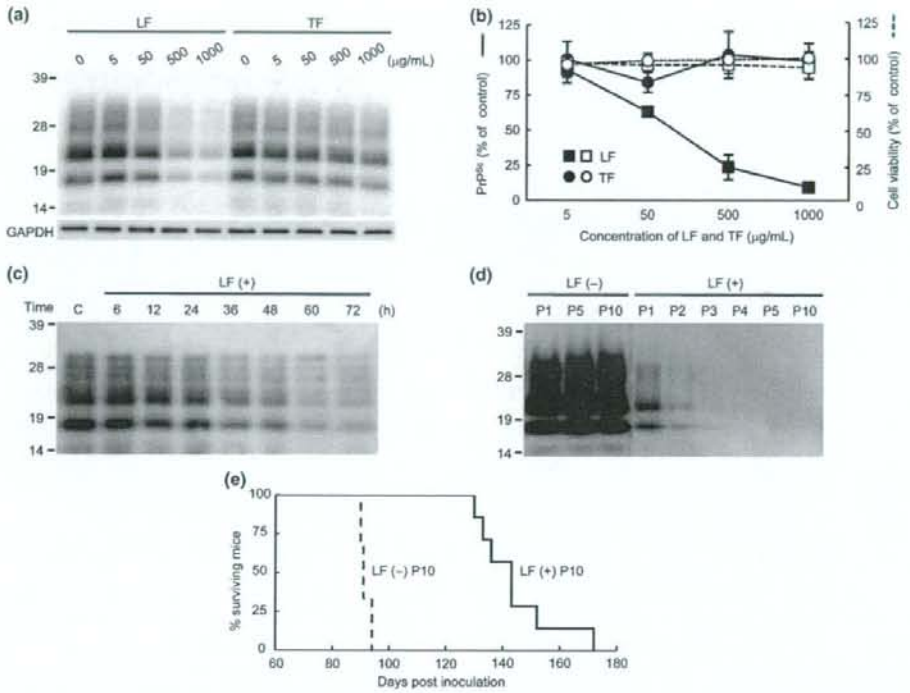

Fig. 1 LF inhibits PrP^{Sc} accumulation and prion replication in ScN2a58 cells. (a) Dose-dependent inhibition of PrP^{Sc} accumulation in ScN2a58 cells by LF. PrP^{Sc} levels in ScN2a58 cells were measured by immunoblot with Mab T2 after 3 days of culture in the absence or presence of LF and TF at the indicated concentrations. Molecular mass standards (kDa) are indicated on the left. (b) The densitometric measurement of PrP^{Sc} signals detected in the immunoblot is shown in the graph (continuous line). The signals of PrP^{Sc} from LF (closed squares) or TF (closed circles)-treated ScN2a58 cells are expressed as a percentage of the signals from untreated cells. Each bar indicates the mean values (± SD) of at least three independent experiments. Cell viability determined by the WST-8 assay is also shown in the same graph (dashed line). The absorbance values from LF (open squares) or TF (open circles)-treated ScN2a58 cells is expressed as a percentage of the absorbance of untreated cells in which the absorbance values indicate the yield of coloured formazan in proportion to the total number of viable cells. Each bar indicates the mean values (± SD) of at least three independent experiments. (c) Kinetics of LF-mediated inhibition of PrP^{Sc} formation. ScN2a58 cells were incubated with 500 μg/mL of LF for an indicated duration (6–72 h) and then rinsed three times with HBSS and cultured further with fresh medium. Four days after plating, the level of PrP^{Sc} in ScN2a58 cells was determined by immunoblot. (d) Inhibition of PrP^{Sc} production in ScN2a58 cells serially passaged 10 times (total 40 days) in the presence or absence of 500 μg/mL of LF. Molecular mass standards (kDa) are indicated on the left. (e) Interference of prion replication in ScN2a58 cells by LF. Tga20 mice were inoculated intracerebrally with ScN2a58 cells in 10 serial passages in the presence or absence of 500 μg/mL of LF. Animals that received LF-treated cells [LF (+) P10] showed statistically significant longer survival times compared to those that received non-treated cells [LF (−) P10] ($p < 0.01$).

amino acid residues 35 and 53, and therefore recognises only full-length PrP (Fig. 2a).

Further, to characterize the effect of LF on the elevation of full-length PrP^{C} levels, we performed several experiments. N2a58 cells were incubated for 3 days in the presence or absence of 500 μg/mL of LF or TF. Following lysis and precipitation by acetone, PrP^{C} present in lysates was analyzed by immunoblot, and semi-quantification was performed by densitometry after removal of carbohydrates with PNGase F. A marked increase in the ratio of full-length PrP^{C} to total PrP^{C} was observed in LF-treated cells compared with non- or TF-treated cells (Fig. 2b and c), while the levels of total PrP in LF-treated cells were almost equivalent to those in non- or TF-treated cells (data not shown). This suggests that an increase in the full-length PrP^{C} levels in LF-treated cells was concomitant with a decrease in the C-terminal fragments levels. An increase in the full-length PrP levels were also observed in ScN2a58 cells treated with LF (Fig. 2d).

Surface retention of full-length PrP^{C} by LF

Full-length PrP^{C} is cleaved to generate C1 fragments along its recycling route between the cell surface and the endosomal compartments (Shyng *et al.* 1993). Thus, the present

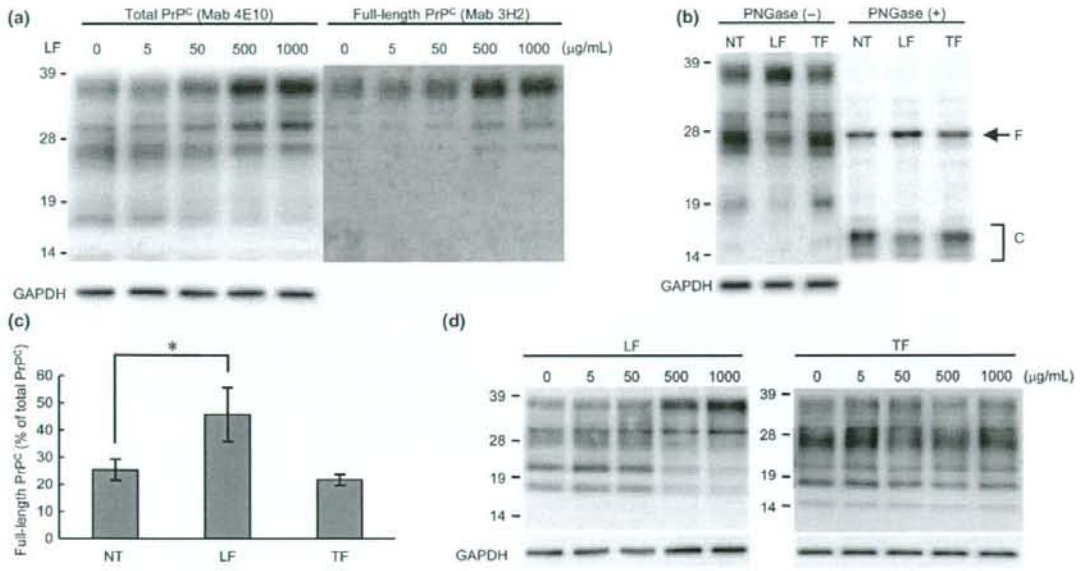

Fig. 2 LF-mediated increase in the ratio of full-length PrP^C to total PrP^C. (a) PrP levels in N2a58 cells were measured by immunoblot after 3 days of culture in the absence or presence of LF at the indicated concentrations without PK treatment. Total PrP^C levels was assayed with Mab 4E10 and full-length PrP^C was assayed with Mab 3H2 reacting with an epitope located in the N-terminus between PrP amino acid residues 35 and 52. Molecular mass standards (kDa) are indicated on the left. GAPDH was used as the control to confirm the protein content in cell extracts. (b) PrP^C levels in N2a58 cells were measured by immunoblot after 3 days of culture in the absence (NT) or presence of 500 μg/mL LF or TF without PK treatment. Proteins in post-nuclear cell extracts prepared without PK treatment were precipitated with acetone prior to electrophoresis. PrP^C present in precipitates were treated with or without PNGaseF and analyzed by immunoblot with Mab 4E10. F represents full-length PrP and C represents C-treminal fragments. (c) Densitometric analysis of full-length PrP^C signals detected in panel b. The signals of full-length PrP^C are expressed as a percentage of the signals from total PrP^C (full-length PrP^C plus C-terminal fragments). Each bar indicates the mean values (±SD) of at least three independent experiments. Significant difference at p-value of <0.05 (·) between LF and non-treated cells is indicated. (d) PrP levels in ScN2a58 cells were measured by immunoblot after 3 days of culture in the presence of LF or TF at the indicated concentrations without PK treatment. Total PrP levels was assayed with Mab T2.

observation of an increase in full-length PrP concomitant with the decrease in the C-terminal fragments levels in LF-treated cells raised the possibility that full-length PrP was retained on the cell surface by LF treatment.

The cell surface expression of PrP^C upon treatment with LF was investigated by fluorescence-activating cell sorting analysis. Mabs 3H2 and SAF32 reacting with linear amino acid epitopes 59–89 were used to detect full-length PrP^C, and Mabs T2 and SAF61 reacting with the discontinuous epitope spanning amino acids 132–156 and the linear amino acid epitopes 142–160, respectively, were used to assess the total surface PrP^C. LF-treated cells showed an increase in the full-length PrP^C levels as compared with untreated cells. On the other hand, there was no significant difference in the total PrP^C levels between untreated and LF-treated cultures (Fig. 3a). The effect of LF on the cellular localization of PrP was also examined by confocal microscopy. To detect only full-length PrP^C, we used N2a58 cells transiently transfected with N-terminally EGFP-fused PrP^C (EGFP-PrP^C). After 24 h of treatment of N2a58 cells with LF, EGFP-PrP^C was found to be mostly localized at the cell surface. On the other hand, in accordance with a previous report (Hachiya *et al.* 2004), EGFP-PrP^C localization was predominant in the intracellular compartment in untreated or TF-treated cells (Fig. 3b).

LF increases full-length PrP^C on the cell surface by diminishing internalization

We next examined whether LF could diminish the internalization of full-length PrP^C on the cell surface. N2a58 cells were cell surface biotinylated via a cleavable disulfide linkage and incubated at 37°C for various times in the presence or absence of LF. Intracellular PrP^C was measured after treatment of the membrane-impermeant thiol-reducing reagent, MesNa. The intracellular PrP levels internalized in the presence or absence of LF is depicted in the immunoblot shown in Fig. 4a. Immunoblot probed with Mab T2 showed that approximately equal amount of PrP^C were blotted on the

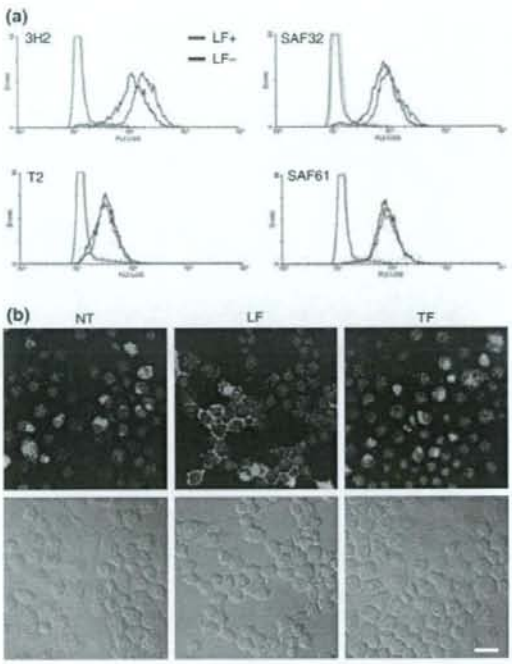

Fig. 3 Full-length surface PrP increases after treatment with LF. (a) Fluorescence-activated cell sorting analysis of cell surface expression levels of PrP^C and full-length PrP^C. The histograms depict the cell surface expression in non-permeabilized cells incubated with 500 μg/mL LF for 24 h. FL2 represents the fluorescence intensity in LF-treated cells (red line) and in the non-treated cells (blue line), plotted against the number of cells (events). For each cell population, 10 000 events were measured. Mabs 3H2 and SAF32 were used for detection of full-length PrP^C, and Mabs T2 and SAF61 and were used for detection of the total PrP^C on the cell surface. (b) Confocal fluorescence microscopic analysis of EGFP-PrP distribution in N2a58 cells. N2a58 cells transiently expressing EGFP-PrP (green) were incubated with 500 μg/mL LF or TF for 24 h. Untreated control N2a58 cells (NT) are also shown. N2a58 cells growing on cover glasses were fixed with 4% paraformaldehyde and confocal fluorescent images (upper panels) and Nomarski differential interference contrast images (lower panels) were obtained. Nuclei were counterstained with TO-PRO-3 (red). Scale bar, 20 μm.

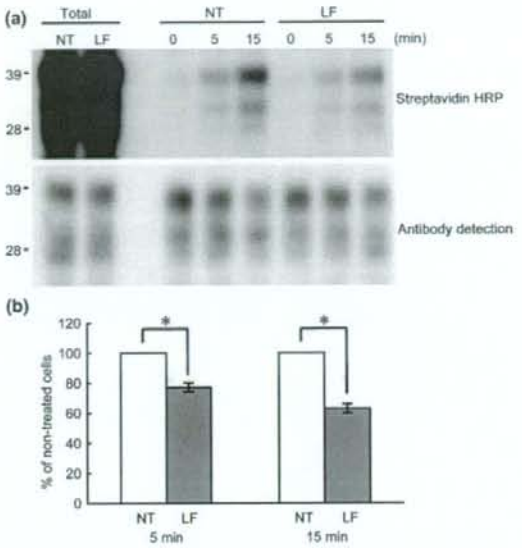

Fig. 4 Intracellular PrP^C internalization in the presence or absence of LF. (a) N2a58 cells were surface biotinylated with Sulfo-NHS-SS-Biotin at 4°C, and incubated at 37°C for 5 or 15 min in the absence (NT) or presence (LF) of 1000 μg/mL LF. Cells were then incubated with MesNa (a small membrane-impermeant thiol-reducing reagent) for 1 h to cleave the disulphide bond in the spacer arm on cell surface. Surface biotinylated-N2a58 cells without incubation at 37°C and MesNa treatment were also prepared (total). PrP^C was immunoprecipitated from cell lysates using anti-PrP Mab 43C5 and immunoblotted with streptavidin-HRP or Mab T2. Molecular mass standards (kDa) are indicated on the left. (b) Densitometric analysis of the internalized PrP^C signals detected in panel a. The signals of internalized PrP^C from LF-treated cells are expressed as a percentage of the signals of PrP^C from non-treated cells. Each bar indicates the mean values (± SD) of at least three independent experiments. Statistical comparisons are versus NT at 5 and 15 min, p-value of <0.01 (*).

membrane, on the other hand, immunoblot probed with streptavidin–HRP showed the time-dependent increase of intracellular PrP^C (Fig. 4a). LF diminished the rate of PrP internalization by approximately 40% at 15 min compared with that of the control (Fig. 4b).

Previous studies have implicated that PrP^C contains four complete octapeptide repeats (PHGG(G/S)WGQ) in its N-terminal half that are capable of binding copper ions (Stockel *et al.* 1998; Viles *et al.* 1999). Copper ions can stimulate endocytosis of PrP^C in neuronal cells by moving PrP^C from detergent-resistant membranes into detergent-soluble regions (Pauly and Harris 1998; Taylor *et al.* 2005). LF has a strong iron-binding capacity that has been implicated in antimicrobial mechanisms. Furthermore, LF binds several metal ions such as copper, manganese and cobalt (Harrington 1992). It is possible that LF-dependent sequestration of copper in the culture medium influences PrP^C localization and PrP^{Sc} accumulation in ScN2a58 cells. However, copper supplementation of the LF-containing culture medium did not substantially affect the LF-induced increase of full-length PrP and reduction of PrP^{Sc} in ScN2a58 cells (data not shown).

Binding of PrP by LF

To address whether LF could directly interact with PrP^C or PrP^{Sc}, magnetic beads coupled to BSA, LF and TF were used in 'pull-down' experiments. Cell lysates and brain extracts were incubated with magnetic beads and immunoblot analyzed following treatment with or without PK. PrP^C from

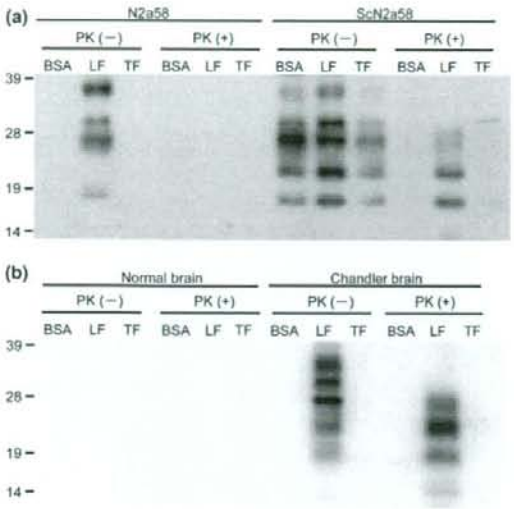

Fig. 5 Interaction of PrP^{C} and PrP^{Sc} with LF. (panels a and b) 'Pull-down' experiments with magnetic beads coupled to BSA, LF, and TF. The extracts of N2a58 or ScN2a58 cells (a) and of brains obtained from non-infected or infected mice (b) were applied to these magnetic beads. Following incubation, the beads were treated with or without proteinase K (PK) and immunoblotted with Mab T2. Molecular mass standards (kDa) are indicated on the left.

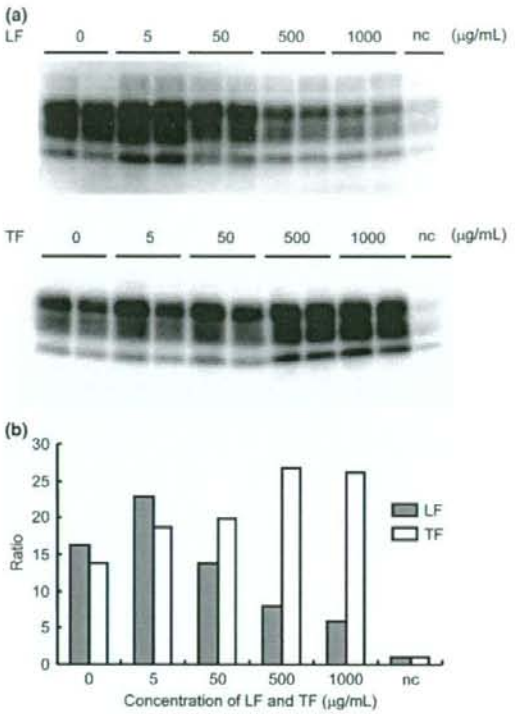

Fig. 6 LF dose-dependent inhibition of PK-resistant PrP formation. (a) Immunoblot analysis of PK-resistant PrP amplified by PMCA. Brain homogenates from mice with Chandler scrapie were added to normal mouse brain homogenates to get final dilutions of 1 : 1000. PMCA was performed on duplicate samples with LF or TF at indicated concentrations. After PK digestion, PK-resistant PrP was detected by immunoblot with Mab T2. (0) represents samples without LF or TF, and (nc) represents samples without amplification. (b) Densitometric analysis of PK-resistant PrP signals in panel a. Each bar represents the average amplification ratio from duplicate samples with (nc) as standard.

N2a58 cells was recovered only from LF-coupled beads, while PrP^{Sc} from ScN2a58 cells was recovered from all the magnetic beads before PK treatment (Fig. 5a). However, obvious PrP^{Sc} signals were detectable only from LF-coupled beads after PK treatment. On the other hand, only LF-coupled beads precipitated PrP^{Sc} from scrapie-infected brain extracts (Fig. 5b). A PrP^{C} signal could be detected from LF-coupled beads in normal brain tissue with prolonged exposure time (data not shown). This observation suggests that LF may have much higher affinity for PrP^{Sc} than PrP^{C} in brain tissues. Alternatively, this could be attributed to the larger PrP^{Sc} levels in scrapie-infected brain tissues compared with ScN2a58 cells.

Inhibition of PK-resistant PrP formation

The ability of LF to directly inhibit PK-resistant PrP formation was examined using the PMCA technique (Murayama *et al.* 2007). Brain homogenates from mice with Chandler scrapie were added to normal mouse brain homogenates, and PMCA was performed in the presence of designated concentrations of LF or TF. LF induced a dose-dependent inhibition of PK-resistant PrP amplification at 50–1000 μg/mL as determined by densitometric analysis (Fig. 6). At a lower concentration (5 μg/mL), LF increased the amount of PK-resistant PrP in PMCA. These results suggest that LF might have biphasic effect on PrP^{Sc}, over-stabilizing PrP^{Sc} at low concentrations. Further studies are needed to address this issue. In contrast, there was a dose-dependent induction of PK-resistant PrP amplification on PMCA in the presence of TF.

Discussion

In this study, we found that the treatment of ScN2a58 cells with LF leads to time- and dose-dependent reduction of PrP^{Sc} levels. LF inhibited PrP^{Sc} accumulation at completely non-toxic concentrations and an IC_{50} of 1.6 μM was obtained. Furthermore, bioassays of LF-treated cells in *tga*20 mice showed the prolonged incubation period compared with non-treated cells, which is indicative of reduced prion infectivity.

Several mechanisms can explain the antiprion activities of LF on infected cells. Since PrP^{Sc} formation is believed to

occur either on the cell surface or along the endocytic pathway (Caughey and Raymond 1991; Caughey *et al.* 1991a; Borchelt *et al.* 1992), in a first hypothesis, LF could inhibit PrP^{Sc} formation in cells by perturbing the cellular trafficking of PrP^{C}. Numerous studies have shown that anti-PrP antibodies are able to inhibit PrP^{Sc} formation in cell culture models. The ability of antibodies to inhibit PrP^{Sc} formation closely relates to efficient binding of antibodies to cell-surface native PrP^{C} leading to a perturbation of PrP cellular trafficking (Kim *et al.* 2004b; Feraudet *et al.* 2005). Furthermore, reduction of laminin receptor precursors/lamin receptors (LPR/LR) expression or the blockage of LPR/LR inhibits PrP^{Sc} formation by blocking of the PrP internalization in ScN2a cells (Leucht *et al.* 2003). In experiments with normal cells treated with LF, we were able to demonstrate that LF is most likely to retain PrP^{C} on the cell-surface by interfering with the PrP^{C} internalization process. Taking these previous and our findings together, we propose that the LF-mediated interference of PrP internalization may reduce the availability of the substrate for PrP^{Sc} formation within endocytic pathway, resulting in a time-dependent reduction in PrP^{Sc}. Further studies are needed to address this issue.

The precise mechanisms by which LF diminishes the internalization of full-length PrP^{C} on the cell surface are unclear. Recent studies have shown that the low-density lipoprotein receptor-related protein (LRP) 1 mediates endocytosis of the PrP^{C} (Taylor and Hooper 2007; Parkyn *et al.* 2008). In these reports, PrP^{C} internalization is inhibited by around 1 μM of receptor-associated protein, a universal competitor for ligand binding to LRP. Since LRP is one of the cell-surface receptor for LF (Takayama *et al.* 2003), it is possible that LF may inhibit PrP^{C} internalization by binding to LRP similarly to receptor-associated protein. The LRP1 mRNA expression in N2a cells was confirmed by reverse-transcriptase-PCR (data not shown). Alternatively, several lines of evidence demonstrate that the N-terminal domain of PrP, in particular, the cluster of basic residues (KKRPKP, residues 23–28) is essential for its internalization (Sunyach *et al.* 2003; Taylor *et al.* 2005). It seems likely that LF interacts with PrP at this polybasic region and prevents its internalization. To examine this possibility, LF was reacted with a gridded array of synthetic peptides comprising 122 polypeptides of 13 amino acids, sequentially shifted by two amino acids and covering the entire mouse PrP sequence (Yokoyama *et al.* 2001). However, LF failed to associate with any of the polypeptides (data not shown), suggesting that LF does not block the N-terminal cluster of basic residues of PrP. It is noteworthy that this observation contradicts our result presented in Fig. 5 demonstrating that LF can interact with both cellular PrP^{C} and PrP^{Sc}. The reason for this discrepancy in the interaction between LF and PrP is unclear. Because PrP is known to interact with numerous cellular factors, such as nucleic acids, sulphated glycosaminoglycans (GAGs), plasminogen and LPR/LR (Gauczynski *et al.* 2001), it is conceivable that LF-PrP binding is indirect and mediated by one or more of the cellular components. Alternatively, the interaction between LF and PrP may require a tertiary structure. More research will be required to determine the precise mechanisms by which LF retains PrP^{C} on the cell surface.

As a second hypothesis about LF-mediated antiprion mechanisms, LF could inhibit the interaction between PrP^{C} and PrP^{Sc} required for PrP^{C} conversion. Our data show that LF could bind to PrP and partially inhibited PK-resistant PrP amplification in the PMCA assay. In our sense, this effect should be rather due to LF/ PrP^{Sc} interaction, since LF appears to have much higher binding affinity to PrP^{Sc} than PrP^{C} in brain tissues (Fig. 5b). Although whether this direct inhibition accounts mechanistically for the inhibition observed in ScN2a58 cells is not clear, it is possible that LF prevent the interaction between PrP^{C} and PrP^{Sc} on the cell surface. In addition, as was seen in the previous study using anti-PrP Mab (Pankiewicz *et al.* 2006), it is possible for LF to enter the cells together with PrP^{Sc} and inhibit PrP^{Sc} formation in the endsomes. Whether LF can internalize together with PrP remains to be determined.

In a third hypothesis for mechanisms by which LF interferes with prion replication, LF could inhibit interaction between cofactors for conversion and PrP^{C} and/or PrP^{Sc}. Endogenous sulphated GAGs such as heparin sulfate have been demonstrated to be cofactors for conversion. On the other hand, it has been proposed that bovine LF directly interacts with cell membrane-associated GAGs (Ishii *et al.* 2007), and the peptide LFB is assumed to be, at least in part, the binding site for GAGs (Shimazaki *et al.* 1998). Thus, it is possible that LF competes with PrP^{C} and/or PrP^{Sc} for binding of GAGs leading to a inhibition of PrP^{Sc} formation. However, we did not observe a reduction in PrP^{Sc} in ScN2a58 cells by LFB treatment. Nevertheless, this observation do not exclude the possibility that other GAGs-binding domains exist in LF and may interfere with the interaction between GAGs and PrP^{C} and/or PrP^{Sc}.

The antiprion activity of LF did not appear to relate to a destabilization of pre-existing PrP^{Sc} aggregates. Incubation of the cell lysates or brain extracts with LF before PK treatment did not reduce PrP^{Sc} immunoblot band intensity (data not shown). On the contrary, LF increased the PK resistance of PrP^{Sc} in both cellular and brain extracts. This observation also excludes another possibility that LF artifactually interferes with the immunoblot detection of PrP^{Sc}.

In summary, we have demonstrated that LF is able to mediate the clearance of PrP^{Sc} and the reduction of prion infectivity in cells persistently infected with prion. The mechanism of action of LF potentially involves the cell-surface retention of PrP and/or binding to PrP. LF is non-toxic and has been reported to cross the blood–brain barrier via receptor-mediated transcytosis in both *in vitro* and *in vivo* models (Fillebeen *et al.* 1999; Ji *et al.* 2006). These obser-

vations may have therapeutic implications of LF for prion diseases, but it is unlikely that an intracerebral LF distribution at concentration (500 μg/mL) that showed antiprion activity in our *in vitro* assay can be attained by systemic administration. However, elucidation of the antiprion mechanisms of LF may contribute not only to the establishment of new class of therapeutic agent but also to comprehension of the prion replication mechanisms. In addition, the high affinity of LF for PrP^{Sc} could be applied for a diagnosis or analytical use of prion diseases. It would be interesting to investigate an underlying cause of the high affinity of LF for PrP^{Sc} and to examine whether LF-derived peptides and/or recombinant LF deletion mutant has affinity for PrP^{Sc}.

Acknowledgments

We are grateful to Dr. N. Nishida for donation of the N2a58 cell line. We thank Dr. M. Horiuchi for the gift of Mab 43C5. We would also like to thank Ms. N. Yamaguchi and Ms. Y. Miyama for their technical assistance. We are grateful to Dr. T. Kuhara for helpful discussions. This study was supported in part by a Grant-in-Aid from the Bovine Spongiform Encephalopathy Control Project of the Ministry of Agriculture, Forestry and Fisheries of Japan and a grant from the Special Coordination Funds for strategic cooperation to control emerging and re-emerging infections from the Ministry of Education, Culture, Sports, Science and Technology, Japan.

References

Arnold R. R., Cole M. F. and McGhee J. R. (1977) A bactericidal effect for human lactoferrin. *Science* **197**, 263–265.

Borchelt D. R., Taraboulos A. and Prusiner S. B. (1992) Evidence for synthesis of scrapie prion proteins in the endocytic pathway. *J. Biol. Chem.* **267**, 16188–16199.

Caughey B. and Raymond G. J. (1991) The scrapie-associated form of PrP is made from a cell surface precursor that is both protease- and phospholipase-sensitive. *J. Biol. Chem.* **266**, 18217–18223.

Caughey B. and Raymond G. J. (1993) Sulfated polyanion inhibition of scrapie-associated PrP accumulation in cultured cells. *J. Virol.* **67**, 643–650.

Caughey B., Raymond G. J., Ernst D. and Race R. E. (1991a) N-terminal truncation of the scrapie-associated form of PrP by lysosomal protease(s): implications regarding the site of conversion of PrP to the protease-resistant state. *J. Virol.* **65**, 6597–6603.

Caughey B. W., Dong A., Bhat K. S., Ernst D., Hayes S. F. and Caughey W. S. (1991b) Secondary structure analysis of the scrapie-associated protein PrP 27-30 in water by infrared spectroscopy. *Biochemistry* **30**, 7672–7680.

Caughey W. S., Raymond L. D., Horiuchi M. and Caughey B. (1998) Inhibition of protease-resistant prion protein formation by porphyrins and phthalocyanines. *Proc. Natl Acad. Sci. USA* **95**, 12117–12122.

Chen S. G., Teplow D. B., Parchi P., Teller J. K., Gambetti P. and Autilio-Gambetti L. (1995) Truncated forms of the human prion protein in normal brain and in prion diseases. *J. Biol. Chem.* **270**, 19173–19180.

Crouch S. P., Slater K. J. and Fletcher J. (1992) Regulation of cytokine release from mononuclear cells by the iron-binding protein lactoferrin. *Blood* **80**, 235–240.

Doh-ura K., Ishikawa K., Murakami-Kubo I., Sasaki K., Mohri S., Race R. and Iwaki T. (2004) Treatment of transmissible spongiform encephalopathy by intraventricular drug infusion in animal models. *J. Virol.* **78**, 4999–5006.

Faucheux B. A., Nillesse N., Damier P. *et al.* (1995) Expression of lactoferrin receptors is increased in the mesencephalon of patients with Parkinson disease. *Proc. Natl Acad. Sci. USA* **92**, 9603–9607.

Feraudet C., Morel N., Simon S., Volland H., Frobert Y., Creminon C., Vilette D., Lehmann S. and Grassi J. (2005) Screening of 145 anti-PrP monoclonal antibodies for their capacity to inhibit PrPSc replication in infected cells. *J. Biol. Chem.* **280**, 11247–11258.

Fillebeen C., Descamps L., Dehouck M. P., Fenart L., Benaissa M., Spik G., Cecchelli R. and Pierce A. (1999) Receptor-mediated transcytosis of lactoferrin through the blood-brain barrier. *J. Biol. Chem.* **274**, 7011–7017.

Forloni G., Iussich S., Awan T. *et al.* (2002) Tetracyclines affect prion infectivity. *Proc. Natl Acad. Sci. USA* **99**, 10849–10854.

Gabizon R., McKinley M. P., Groth D. and Prusiner S. B. (1988) Immunoaffinity purification and neutralization of scrapie prion infectivity. *Proc. Natl Acad. Sci. USA* **85**, 6617–6621.

Gauczynski S., Peyrin J. M., Haik S. *et al.* (2001) The 37-kDa/67-kDa laminin receptor acts as the cell-surface receptor for the cellular prion protein. *EMBO J.* **20**, 5863–5875.

Hachiya N. S., Watanabe K., Sakasegawa Y. and Kaneko K. (2004) Microtubules-associated intracellular localization of the NH2-terminal cellular prion protein fragment. *Biochem. Biophys. Res. Commun.* **313**, 818–823.

Harrington J. P. (1992) Spectroscopic analysis of the unfolding of transition metal-ion complexes of human lactoferrin and transferrin. *Int J. Biochem.* **24**, 275–280.

Harris D. A., Huber M. T., van Dijken P., Shyng S. L., Chait B. T. and Wang R. (1993) Processing of a cellular prion protein: identification of N- and C-terminal cleavage sites. *Biochemistry* **32**, 1009–1016.

Ishii T., Ishimori H., Mori K., Uto T., Fukuda K., Urashima T. and Nishimura M. (2007) Bovine lactoferrin stimulates anchorage-independent cell growth via membrane-associated chondroitin sulfate and heparan sulfate proteoglycans in PC12 cells. *J. Pharmacol. Sci.* **104**, 366–373.

Iwamaru Y., Takenouchi T., Ogihara K. *et al.* (2007) Microglial cell line established from prion protein-overexpressing mice is susceptible to various murine prion strains. *J. Virol.* **81**, 1524–1547.

Ji B., Maeda J., Higuchi M., Inoue K., Akita H., Harashima H. and Suhara T. (2006) Pharmacokinetics and brain uptake of lactoferrin in rats. *Life Sci.* **78**, 851–855.

Kawamata T., Tooyama I., Yamada T., Walker D. G. and McGeer P. L. (1993) Lactotransferrin immunocytochemistry in Alzheimer and normal human brain. *Am. J. Pathol.* **142**, 1574–1585.

Kim C. L., Umetani A., Matsui T., Ishiguro N., Shinagawa M. and Horiuchi M. (2004a) Antigenic characterization of an abnormal isoform of prion protein using a new diverse panel of monoclonal antibodies. *Virology* **320**, 40–51.

Kim C. L., Karino A., Ishiguro N., Shinagawa M., Sato M. and Horiuchi M. (2004b) Cell-surface retention of PrPC by anti-PrP antibody prevents protease-resistant PrP formation. *J. Gen. Virol.* **85**, 3473–3482.

Leucht C., Simoneau S., Rey C., Vana K., Rieger R., Lasmezas C. I. and Weiss S. (2003) The 37 kDa/67 kDa laminin receptor is required for PrP(Sc) propagation in scrapie-infected neuronal cells. *EMBO Rep.* **4**, 290–295.

Leveugle B., Spik G., Perl D. P., Bouras C., Fillit H. M. and Hof P. R. (1994) The iron-binding protein lactotransferrin is present in pathologic lesions in a variety of neurodegenerative disorders: a comparative immunohistochemical analysis. *Brain Res.* **650**, 20–31.

May B. C., Fafarman A. T., Hong S. B., Rogers M., Deady L. W., Prusiner S. B. and Cohen F. E. (2003) Potent inhibition of scrapie prion replication in cultured cells by bis-acridines. *Proc. Natl Acad. Sci. USA* **100**, 3416–34121.

Murayama Y., Yoshioka M., Yokoyama T., Iwamaru Y., Imamura M., Masujin K., Yoshiba S. and Mohri S. (2007) Efficient in vitro amplification of a mouse-adapted scrapie prion protein. *Neurosci. Lett.* **413**, 270–273.

Nishida N., Harris D. A., Vilette D., Laude H., Frobert Y., Grassi J., Casanova D., Milhavet O. and Lehmann S. (2000) Successful transmission of three mouse-adapted scrapie strains to murine neuroblastoma cell lines overexpressing wild-type mouse prion protein. *J. Virol.* **74**, 320–325.

Pan K. M., Baldwin M., Nguyen J. *et al.* (1993) Conversion of alpha-helices into beta-sheets features in the formation of the scrapie prion proteins. *Proc. Natl Acad. Sci. USA* **90**, 10962–10966.

Pankiewicz J., Prelli F., Sy M. S., Kascsak R. J., Kascsak R. B., Spinner D. S., Carp R. I., Meeker H. C., Sadowski M. and Wisniewski T. (2006) Clearance and prevention of prion infection in cell culture by anti-PrP antibodies. *Eur. J. Neurosci.* **23**, 2635–2647.

Parkyn C. J., Vermeulen E. G., Mootoosamy R. C. *et al.* (2008) LRP1 controls biosynthetic and endocytic trafficking of neuronal prion protein. *J. Cell Sci.* **121**, 773–783.

Pauly P. C. and Harris D. A. (1998) Copper stimulates endocytosis of the prion protein. *J. Biol. Chem.* **273**, 33107–33110.

Pocchiari M., Schmittinger S. and Masullo C. (1987) Amphotericin B delays the incubation period of scrapie in intracerebrally inoculated hamsters. *J. Gen. Virol.* **68**, 219–223.

Prusiner S. B. (1982) Novel proteinaceous infectious particles cause scrapie. *Science* **216**, 136–144.

Prusiner S. B. (1991) Molecular biology of prion diseases. *Science* **252**, 1515–1522.

Schmidt A., Hannah M. J. and Huttner W. B. (1997) Synaptic-like microvesicles of neuroendocrine cells originate from a novel compartment that is continuous with the plasma membrane and devoid of transferrin receptor. *J. Cell Biol.* **137**, 445–458.

Shimazaki K., Tazume T., Uji K., Tanaka M., Kumura H., Mikawa K. and Shimo-Oka T. (1998) Properties of a heparin-binding peptide derived from bovine lactoferrin. *J. Dairy Sci.* **81**, 2841–2849.

Shyng S. L., Huber M. T. and Harris D. A. (1993) A prion protein cycles between the cell surface and an endocytic compartment in cultured neuroblastoma cells. *J. Biol. Chem.* **268**, 15922–15928.

Stockel J., Safar J., Wallace A. C., Cohen F. E. and Prusiner S. B. (1998) Prion protein selectively binds copper(II) ions. *Biochemistry.* **37**, 7185–7193.

van der Strate B. W., Beljaars L., Molema G., Harmsen M. C. and Meijer D. K. (2001) Antiviral activities of lactoferrin. *Antiviral Res.* **52**, 225–239.

Sunyach C., Jen A., Deng J., Fitzgerald K. T., Frobert Y., Grassi J., McCaffrey M. W. and Morris R. (2003) The mechanism of internalization of glycosylphosphatidylinositol-anchored prion protein. *EMBO J.* **22**, 3591–3601.

Supattapone S., Nguyen H. O., Cohen F. E., Prusiner S. B. and Scott M. R. (1999) Elimination of prions by branched polyamines and implications for therapeutics. *Proc. Natl Acad. Sci. USA* **96**, 14529–14534.

Takase K. (1998) Reactions of denatured proteins with other cellular components to form insoluble aggregates and protection by lactoferrin. *FEBS Lett.* **441**, 271–274.

Takayama Y., Takahashi H., Mizumachi K. and Takezawa T. (2003) Low density lipoprotein receptor-related protein (LRP) is required for lactoferrin-enhanced collagen gel contractile activity of human fibroblasts. *J. Biol. Chem.* **278**, 22112–22118.

Taylor D. R. and Hooper N. M. (2007) The low-density lipoprotein receptor-related protein 1 (LRP1) mediates the endocytosis of the cellular prion protein. *Biochem. J.* **402**, 17–23.

Taylor D. R., Watt N. T., Perera W. S. and Hooper N. M. (2005) Assigning functions to distinct regions of the N-terminus of the prion protein that are involved in its copper-stimulated, clathrin-dependent endocytosis. *J. Cell Sci.* **118**, 5141–5153.

Viles J. H., Cohen F. E., Prusiner S. B., Goodin D. B., Wright P. E. and Dyson H. J. (1999) Copper binding to the prion protein: structural implications of four identical cooperative binding sites. *Proc. Natl Acad. Sci. USA* **96**, 2042–2047.

Yokoyama T., Kimura K. M., Ushiki Y., Yamada S., Morooka A., Nakashiba T., Sassa T. and Itohara S. (2001) In vivo conversion of cellular prion protein to pathogenic isoforms, as monitored by conformation-specific antibodies. *J. Biol. Chem.* **276**, 11265–11271.

